EUROPEAN RESPIRATORY *journal*

FLAGSHIP SCIENTIFIC JOURNAL OF ERS

Early View

Original article

Connexin 43 Is a Promising Target for Pulmonary Hypertension due To Hypoxemic Lung Disease

Claire Bouvard, Nafiisha Genet, Carole Phan, Baptiste Rode, Raphaël Thuillet, Ly Tu, Paul Robillard, Marilyne Campagnac, Raffaella Soleti, Eric Dumas De La Roque, Frédéric Delcambre, Laurent Cronier, Thibaud Parpaite, Elise Maurat, Patrick Berger, Jean-Pierre Savineau, Roger Marthan, Christophe Guignabert, Véronique Freund-Michel, Christelle Guibert

Please cite this article as: Bouvard C, Genet N, Phan C, *et al*. Connexin 43 Is a Promising Target for Pulmonary Hypertension due To Hypoxemic Lung Disease. *Eur Respir J* 2019; in press (https://doi.org/10.1183/13993003.00169-2019).

This manuscript has recently been accepted for publication in the *European Respiratory Journal*. It is published here in its accepted form prior to copyediting and typesetting by our production team. After these production processes are complete and the authors have approved the resulting proofs, the article will move to the latest issue of the ERJ online.

Connexin 43 Is a Promising Target for Pulmonary Hypertension due To Hypoxemic Lung Disease

Claire Bouvard[1, 2], Nafiisha Genet[1, 2], Carole Phan[5, 6], Baptiste Rode[1, 2], Raphaël Thuillet[5, 6], Ly Tu[5, 6], Paul Robillard[1, 2], Marilyne Campagnac[1, 2], Raffaella Soleti[7], Eric Dumas De La Roque[1, 3], Frédéric Delcambre[3], Laurent Cronier[4], Thibaud Parpaite[1, 2], Elise Maurat[1, 2], Patrick Berger[1, 2, 3], Jean-Pierre Savineau[1, 2], Roger Marthan[1, 2, 3], Christophe Guignabert[5, 6], Véronique Freund-Michel[1, 2], Christelle Guibert[1, 2, #]

[1] INSERM, Centre de recherche Cardio-Thoracique de Bordeaux, U1045, F-33604 Pessac, France; [2] Univ. Bordeaux, Centre de recherche Cardio-Thoracique de Bordeaux, U1045, F-33000, Bordeaux, France; [3] CHU de Bordeaux, F-33604 Pessac, France; [4] Laboratoire Signalisation et Transports Ioniques Membranaires, CNRS ERL 7003, Université de Poitiers, F-86073 Poitiers, France ; [5] INSERM UMR_S 999, F-92350 Le Plessis-Robinson, France; [6] Université Paris-Sud, Université Paris-Saclay, F-94270 Le Kremlin-Bicêtre, France; [7] Laboratoire Stress oxydant et pathologies métaboliques, INSERM U1063, F-49100 Angers, France.

Running title: Contribution of Cx43 to pulmonary hypertension

Manuscript word count: 3543

 # Address Correspondence to:
Christelle GUIBERT, PhD;
Centre de Recherche Cardio-Thoracique de Bordeaux, INSERM U1045;
Plateforme Technologique d'Innovation Biomédicale (PTIB)
Hôpital Xavier Arnozan
Avenue du Haut Lévêque
33604 Pessac Cedex, France
Tel: +33 5 47 30 27 52
E-mail: christelle.guibert@u-bordeaux.fr

“take-home” message

Connexin43 (Cx43), part of intercellular channels, is increased in patients with hypoxia-induced pulmonary hypertension (CH-PH) and is crucial in lung inflammation and pulmonary artery remodelling in mice with CH-PH suggesting Cx43 as a therapeutic option.

Abstract

The mechanisms underlying pulmonary hypertension (PH) are complex and multifactorial and involve different cell types that are interconnected through gap junctional channels. Although connexin (Cx)-43 is the most abundant gap junction protein in heart and lungs and critically governs intercellular signalling communication, its contribution to PH remains unknown. The focus of the present study is thus to evaluate Cx43 as a potential new target in PH.

Expressions of Cx37, Cx40, and Cx43 were studied in lung specimens from patients with idiopathic pulmonary arterial hypertension (iPAH) or PH associated to hypoxemic chronic lung diseases (CH-PH). Heterozygous Cx43 knockdown CD1 ($Cx43^{+/-}$) and wild-type littermate ($Cx43^{+/+}$) mice at 12 weeks of age were randomly divided into two groups, one of which was maintained in room air and the other exposed to hypoxia (10% O_2) for 3 weeks. We evaluated pulmonary haemodynamics, remodelling processes in cardiac tissues and pulmonary arteries (PA), lung inflammation, and PA vasoreactivity.

Cx43 levels were increased in PA from CH-PH patients, whereas Cx43 levels decreased in PA from iPAH patients. No difference in Cx37 or Cx40 was noted. Upon hypoxia treatment, the $Cx43^{+/-}$ mice were partially protected against chronic hypoxia-induced PH when compared to $Cx43^{+/+}$ mice, with reduced pulmonary arterial muscularisation and inflammatory infiltration. Interestingly, the adaptive changes in cardiac remodelling in $Cx43^{+/-}$ mice were not affected. PA contraction to endothelin-1 was increased in $Cx43^{+/-}$ under normoxic and hypoxic conditions.

Taken together, these results indicate that targeting Cx43 may have beneficial therapeutic effects in PH without affecting compensatory cardiac hypertrophy.

Key words: Pulmonary hypertension, chronic hypoxia, therapeutic target, gap junction proteins, Connexin 43.

Introduction

Pulmonary hypertension (PH) encompasses a group of devastating cardiovascular diseases with high morbidity and mortality, comprising idiopathic pulmonary hypertension (iPAH) and forms of PH associated with cardiopulmonary diseases such as hypoxemic chronic lung diseases (chronic hypoxic PH or CH-PH) [1]. All forms of PH are characterized by progressive remodelling of distal pulmonary arteries and vasoconstriction/relaxation imbalance leading to sustained elevated mean pulmonary arterial pressure over 25 mmHg at rest. As a consequence, hypertrophic and failing right heart is responsible for premature patient death [2, 3]. Recent evidence also points out the importance of inflammation in all forms of PH [4, 5]. PH is still incurable and lung transplantation is too often the only therapeutic option with a survival rate of 52-75 % at 5 years after surgery [1]. Moreover, treatment for CH-PH is currently based on drugs developed for iPAH without clear evidence of their efficacy on CH-PH [1]. PH and CH-PH thus remain an important challenge and development of new drugs specific to different PH forms may be a key point.

In PH, two essential actors are involved in pulmonary artery (PA) dysfunction: pulmonary artery endothelial cells (PA-EC) and smooth muscle cells (PA-SMC) [6]. Under physiological conditions, PA-EC and PA-SMC are responsible for a fine control of PA tone through a subtle crosstalk involving direct myoendothelial communications (gap junctions) [7]. Gap junctions are clusters of intercellular channels composed of various structural proteins (connexins; Cx) also essential for spreading cellular signalling [7, 8]. Our group and others have previously shown that Cx37, 40 and 43 are expressed in rat, mouse and human PA and such expression is modified in experimental models of PH as well as in patients with iPAH but disparities have been observed between the different studies [8-14]. Interestingly, in vessels, Cx43 is known to

be involved in tone regulation, cell proliferation and inflammatory infiltration which are the main hallmarks of PH [7, 8, 10, 15-17].

In cardiac tissue, Cx40, 43 and 45 are expressed, Cx43 being the most abundant. Moreover, Cx43 expression and localization are modified in hypertrophic cardiac pathologies including in the right ventricle (RV) hypertrophy in the well-established monocrotaline-induced rat model of PH [18-20]. However, so far, cardiac Cx43 expression has not been studied in CH-PH.

We hypothesized that Cx43 may contribute to PH and especially CH-PH. With heterozygous Cx43 knock-down mice ($Cx43^{+/-}$), we addressed the expression and the role of Cx43 on PA reactivity, remodelling processes in cardiac tissues and PA and lung inflammation in an experimental model of CH-PH. From a translational point of view, we also evaluated Cx43 expression in human PH such as CH-PH as well as iPAH to examine the relative specificity of changes in these two severe clinical entities.

Methods

Further details and full description of all methods are provided in the online supplement.

Human material

For the *in vitro* and *in situ* studies, we used lung specimens obtained during lung transplantation from patients with iPAH or CH-PH. The 6 patients with CH-PH had the following diseases associated to PH: emphysema, Kartagener syndrome, cystic fibrosis, familial iPAH (with severe hypoxemia – PO_2 = 59 mm Hg), pulmonary veno-occlusive disease and cystic lung disease. The mean age of the patients was 51.3 ± 6.6 years and

included 3 women and 3 men. The mean of the mean pulmonary arterial pressure was 43.5 ± 2.6 mm Hg. Vessels used were intrapulmonary arteries of the second and third order. Control lung tissue (intrapulmonary arteries) was obtained during lobectomy or pneumonectomy for localized lung cancer. Preoperative cardiological evaluation including echocardiography was performed in the controls to rule out PH, and the lung specimens from the controls were collected at a distance from tumour foci. PA-SMC exposed to *in vitro* chronic hypoxia (figure S2) were obtained from extra-pulmonary arteries of healthy lung donors during lung transplantation. The study was approved by local ethics committees (Comité de Protection des Personnes, Sud-Ouest et Outre-mer III, Bordeaux, France; and Comité de Protection des Personnes, Ile de France VII, Le Kremlin-Bicêtre, France). Informed consent was obtained from each individual patient.

Isolation, culture, and treatment of Human pulmonary vascular cells

Human pulmonary microvascular endothelial cells (PM-EC) and PA-SMC were obtained and cultured as previously described [5, 21-23]. PA-SMC were exposed to chronic hypoxia *in vitro* (1% O_{2-} "Chronic Hypoxia" – CH group) as previously described [24]. PA-SMC of control group ("Normoxia" - N) were exposed to a gas mixture containing 21 % O_2, 74 % N_2, and 5 % CO_2.

Cells were used between passages 3 and 6. Further details are provided in the online supplement.

Animal experiments

All animal studies conformed to the Declaration of Helsinki conventions for the use and care of animals. Agreement (number A33-063-907) was obtained from the French authorities and

all protocols used were approved by the local ethics committee (Comité d'éthique de Bordeaux n° 50, protocol number APAFIS#9212-2017031018562273 v5). Genetically modified adult male CD1 mice (8 - 12 weeks) ($Gja1^{tm1Kdr}$; Jackson Laboratory, Bar Harbor, ME) were used and compared to their wild type littermates. Mutation is due to the in-frame insertion of a promoterless neomycin (Neo) gene into exon 2 of Cx43 (Gja1) gene [25]. $Gja1^{tm1Kdr}$ homozygous ($Cx43^{-/-}$) mice die at birth due to a severe heart defect [25]. Consequently, only heterozygous ($Cx43^{+/-}$) and wild-type ($Cx43^{+/+}$) mice were used for the study. PH was induced by exposing mice to chronic hypoxia (CH) in a hypobaric chamber (380 mmHg) during 21 days while control animals were kept under normobaric N (room air). Number of mice used is specified in the legend of the figures for each set of experiments. Further details are provided in the online supplement.

Statistical analysis

All data are expressed as mean ± SEM of n independent observations. Two-way analysis of variance was used to compare concentration-response curves. Mann-Whitney test was used when comparing two groups. For all other parameters, one-way analysis of variance was used to assess differences among groups, followed by adapted *post hoc* tests (Dunn tests). $P<0.05$ was considered significant. Analyses were performed using GraphPad Prism version 6.07 (Graphpad Software, La Jolla, CA).

Results

Cx43 expression varies in the pulmonary arterial vascular bed in experimental and human PH

Cx43 protein levels were increased in PA from patients with CH-PH (figure 1a). Interestingly, Cx43 expression was inversely decreased in human PA-SMC whereas it was not modified in PM-EC from patients with iPAH compared to control patients (figure 1b, 1c respectively). Consistent with these findings, lung section staining showed a strong increase in Cx43 expression in the smooth muscle of PA from patients with CH-PH compared to patients with iPAH or to control patients (figure 2 and S1). Moreover, when PA-SMC from control patients were exposed to CH (1% O_2 for 48 h), Cx43 mRNA levels were increased (figure S2) suggesting that hypoxia may be responsible for the increased Cx43 expression in PA from CH-PH patients.

Cx40 protein expression seemed unchanged in CH-PH and iPAH patients (figure S3, right images), whereas Cx37 protein expression appeared to be decreased in PA-SMC from iPAH patients and unchanged in PA-SMC from CH-PH patients (figure S3, left images).

In $Cx43^{+/+}$ and $Cx43^{+/-}$ mice, expression of both Cx43 mRNA and protein was similar in PA from N mice compared to CH-PH mice (figure 3a and 3b). Interestingly, Cx43 expression seems to be more present close to the plasma membrane in CH-PH $Cx43^{+/+}$ mice compared to N $Cx43^{+/+}$ mice (figure S4). As expected, in $Cx43^{+/-}$, expression of both Cx43 mRNA and protein was significantly decreased in N as well as CH conditions (figure 3a and 3b, $*P<0.05$, $**P<0.01$, $***P<0.001$). Immunofluorescence assays revealed that Cx43 was expressed in the media (between the two elastic lamina in green, figure 3c and S5) in N and CH conditions in $Cx43^{+/+}$ mice. These experiments also confirmed the decrease of Cx43 in $Cx43^{+/-}$ mice (figure 3c and S5). In accordance with the previous results, mRNA levels for Cx37 and Cx40 were not significantly different between the four experimental groups of mice (figure S6 a and b

respectively) thus suggesting that the decrease in Cx43 in $Cx43^{+/-}$ mice is not compensated by any modification of the Cx37 and/or Cx40 expression.

Role of Cx43 in pulmonary vascular remodelling and right ventricular hypertrophy in mice chronically exposed to hypoxia

By using haematoxylin-eosin staining, we observed a significant increase of the pulmonary arterial wall thickness in $Cx43^{+/+}$ mice with CH-PH that was not present in $Cx43^{+/-}$ mice with CH-PH (figure 4a and 4b). Consistently, PCNA (proliferating cell nuclear antigen) expression that labels proliferating cells was increased only in PA (smooth muscle cells and endothelial cells) from $Cx43^{+/+}$ mice with CH-PH (figure 4c and 4d). No TUNEL-positive cells were detected in PA from lung sections of the four experimental groups of mice whereas few TUNEL-positive cells were detected in mouse colon used as a positive control (figure 4e). Thus, $Cx43^{+/-}$ mice were protected against cell proliferation and intrapulmonary artery remodelling associated to CH-PH.

In contrast in the heart, right ventricular systolic pressure was significantly increased in both $Cx43^{+/+}$ and $Cx43^{+/-}$ mice with CH-PH ($P<0.001$, figure 4f). Moreover, as assessed by Fulton index, right ventricular hypertrophy, a hallmark of right ventricular remodelling in PH, was also present in CH-PH in both $Cx43^{+/+}$ and $Cx43^{+/-}$ mice ($P<0.001$, figure 4g). Interestingly, its magnitude was significantly smaller in $Cx43^{+/-}$ mice compared to $Cx43^{+/+}$ mice ($P<0.05$, figure 4g). As assessed by echocardiography, pulmonary artery acceleration time (PAAT) is similarly decreased in $Cx43^{+/+}$ and $Cx43^{+/-}$ in CH conditions (figure S7 a and b) confirming that right ventricular function is similarly modified in $Cx43^{+/+}$ and $Cx43^{+/-}$ in CH conditions (figure 4f and 4g). Heart rate measured by pulsed-wave Doppler, was similar in all groups of mice (figure S7c). We also performed CD31 immunofluorescent staining and TUNEL experiments to measure capillary density and apoptosis, respectively, in hearts of all groups of mice (figure S8). In all groups of mice, capillary density was similar (figure S8a and b) and

right heart apoptosis was absent (figure S8c) suggesting that heart modifications observed in $Cx43^{+/-}$ are interestingly not strongly deleterious.

Knocking down of Cx43 prevents hypoxia-induced lung inflammation in mice

Inflammatory cells infiltration was estimated with CD45 expression assessed by Western blot and immunofluorescent labelling. CD45 expression was significantly increased (P<0.001) in $Cx43^{+/+}$ mice with CH-PH whereas it was almost absent in $Cx43^{+/-}$ mice (figure 5a and S9). Consistent with this finding, the number of inflammatory cells was increased in $Cx43^{+/+}$ mice with CH-PH (figure 5 b5 and 5 b6 and S9) while such inflammatory process was not present in $Cx43^{+/-}$ mice with CH-PH (figure 5 b7 and 5 b8 and S9). Interestingly, CD45 immunofluorescent staining was localized at the perivascular level of lung sections (figure S9). Altogether, these findings indicate $Cx43^{+/-}$ mice with CH-PH are protected from lung inflammation induced by chronic hypoxia.

Pulmonary arterial contraction and relaxation in $Cx43^{+/+}$ and $Cx43^{+/-}$ mice

We then examined pulmonary arterial reactivity to contractile and relaxant agonists in PA from $Cx43^{+/+}$ and $Cx43^{+/-}$ mice under N and CH conditions. In $Cx43^{+/-}$ compared to $Cx43^{+/+}$ mice, the contraction response curve to endothelin-1 (ET-1) was shifted to the left in N conditions and the maximal response was increased in CH conditions (figure 6a left and right respectively). Moreover, following blockade of endothelin receptors with bosentan 20 mg/kg *in vivo*, carbachol 10 µM had a significant effect only in $Cx43^{+/-}$ mice in CH conditions confirming that endothelin-1 contribution to vasotonus is more important in $Cx43^{+/-}$ mice compared to $Cx43^{+/+}$ in CH conditions (figure S10).

Contraction response curves to serotonin (5-HT) were identical in $Cx43^{+/+}$ and $Cx43^{+/-}$ mice in both N and CH conditions (figure 6b). The maximal contractile response to phenylephrine

was significantly decreased in $Cx43^{+/-}$ mice compared to $Cx43^{+/+}$ mice in N conditions (P<0.01, figure 6c left) whereas it was significantly increased in $Cx43^{+/-}$ mice compared to $Cx43^{+/+}$ mice in CH conditions (P<0.05, figure 6c right). Finally, relaxation to carbachol was identical in $Cx43^{+/-}$ and $Cx43^{+/+}$ mice in N or CH conditions (figure 6d left and right respectively). Interestingly, CH condition strongly reduced relaxation in both $Cx43^{+/-}$ and $Cx43^{+/+}$ mice compared to N condition, suggesting the existence of an endothelial dysfunction in CH-PH as previously described [26]. Von Willebrand factor (vWF) (a marker of endothelium) labelling did not show any obvious endothelial damage in PA from all groups of mice indicating that endothelium damage could not explain the endothelial dysfunction.

Cx43 expression in right and left ventricles in mice

We then compared Cx43 expression in right versus left heart ventricles from all experimental groups of mice. Both Cx43 mRNA and protein were similarly expressed in right and left heart ventricles from $Cx43^{+/+}$ mice under N and CH conditions (figure 7). As expected, Cx43 mRNA and protein were significantly decreased in $Cx43^{+/-}$ mice compared to $Cx43^{+/+}$ mice, under both N and CH conditions (figure 7). As in $Cx43^{+/+}$ mice, both Cx43 mRNA and protein were similarly expressed in right and left heart ventricles from $Cx43^{+/-}$ mice under N and CH conditions (figure 7). Moreover, mRNA levels for Cx37 and Cx40 were not significantly different between the four experimental groups of mice in both right and left heart ventricles (figure S11 a and b respectively) confirming that, as in PA, there was no compensation of the partial Cx43 deletion by Cx37 or 40 altered expression in the heart.

Discussion

In the present study, we provide the first complete description of the deleterious effects of Cx43 in CH-PH in mice. We show that decrease in Cx43 expression attenuates CH-induced PA remodelling and lung inflammation. Partial decrease of Cx43 protein expression also modifies PA vasoreactivity, another important characteristic of PH. Likewise, in human CH-PH, Cx43 protein expression varies and this variation is specific to the PH form (i.e. CH-PH *vs* iPAH), supporting a specific role of Cx43 according to the PH form. We thus suggest that Cx43 may be a promising therapeutic option to be considered in particular for CH-PH that lacks specific treatments [1]. Further work will need to be performed in animal models *in vivo* in order to check the beneficial role of blocking Cx43.

In patients with CH-PH, we clearly demonstrated, for the first time, an important increase in Cx43 protein levels. In patients with iPAH, Cx43 expression was decreased in PA-SMC whereas it was not changed in PM-EC supporting that the vascular Cx43 protein levels is a distinctive characteristic of these two severe forms of PH. Although such experiments have never been performed previously on these human cells, it has been consistently shown that Cx43 protein is decreased in blood-derived endothelial-like cells in patients with iPAH [27]. Likewise, the expression of Cx37 and 40, two other Cx commonly expressed in resistant vessels [28], is also decreased in lung tissues and in PA-EC from patients with iPAH [12]. Consistently, we observed that Cx37 expression tends to decrease in PA-SMC from patients with iPAH. In addition, we showed in the present study that 1% O_2 during 48h induced a fivefold increase of the amount of Cx43 mRNA in cultured PA-SMC from control patients indicating that hypoxia may be responsible for Cx43 protein increase in PA from patients with

CH-PH. Such Cx43 sensitivity to hypoxia has already been shown in the systemic circulation, specifically in cultured smooth muscle cells from rat thoracic aorta exposed to 2% O_2 during 6 hours [29]. Therefore, our study indicates that hypoxia may explain the difference in Cx43 PA expression between patients with CH-PH *versus* iPAH. In the present study, we have not addressed the mechanisms involved in the hypoxia-induced Cx43 regulation but, a previous study showed that HIF-1α is able to increase Cx43 expression through the activation of HRE-5 present in the Cx43 promoter region in human melanoma cell lines [30]. We can thus speculate that such mechanism could be responsible for the hypoxia-induced Cx43 increase in human PA (figure 1a, 2, S1 and S2).

Some of our results regarding Cx expression conflict with previous studies. For instance, we observed similar Cx43 expression in N and CH conditions, and similar Cx37 and 40 mRNA levels in $Cx43^{+/+}$ *versus* $Cx43^{+/-}$ mice independently of the conditions tested (N or CH) in both PA and heart (figure S6 and S11) indicating that Cx43 knock-down was not compensated by variations in expression of connexins with a homology close to Cx43 and expressed in mice PA. However, Htet et al. demonstrated (i) a decrease of Cx43 mRNA expression in PA from both $Cx43^{+/+}$ and $Cx43^{+/-}$ mice with CH-PH compared to N mice and (ii) a decrease of Cx37 and Cx40 mRNA expressions in N $Cx43^{+/-}$ mice compared to N $Cx43^{+/+}$ mice but they used a C57BL6 mouse strain whereas we used a CD1 mouse strain and they induced chronic hypoxia during 14 days whereas we induced chronic hypoxia during 21 days [11].

Moreover, it should be noted that although Cx43 expression is increased in human PA (figure 1a, 2, S1 and S2) this is not the case in mice PA (figure 3). However, Cx43 protein expression has been quantified by performing Western Blot experiments on whole intrapulmonary arteries from mice therefore we detected Cx43 from cytosol as well as from all cellular membranes. Interestingly, Cx43 expression seems to be more present close to the plasma

membrane in CH-PH $Cx43^{+/+}$ mice compared to N $Cx43^{+/+}$ mice (figure S4). Such results could explain discrepancy between Western Blot experiments on human PA and mice PA. Moreover, functional Cx43 is phosphorylated and we can thus speculate that although the total amount of Cx43 is similar in normoxic and hypoxic conditions, the phosphorylation state of Cx43 could be higher in hypoxic conditions in mice.

In $Cx43^{+/+}$ mice, PA remodelling, characterized by smooth muscle and endothelial cell proliferation, and inflammation revealed by immune cells infiltration, were observed in CH conditions (figure 4 and 5). In contrast, in $Cx43^{+/-}$ mice with CH-PH, such processes did not appear suggesting that blocking Cx43 would have a beneficial effect in CH-PH. Since Cx43 is known to be decreased in hypertrophic right ventricle in a classical monocrotaline PH model in rat [19, 20, 31] and $Cx43^{-/-}$ mice are lethal at birth due to an abnormal right ventricular outflow tract from the heart [25], one would expect a harmful heart effect when blocking Cx43. In fact, both right ventricular systolic pressure and hypertrophy were similarly increased in $Cx43^{+/+}$ and $Cx43^{+/-}$ with CH-PH (figure 4f and 4g respectively). However, it should be noted that the increase in right ventricular hypertrophy (assessed by Fulton index) was significantly smaller in $Cx43^{+/-}$ mice compared to $Cx43^{+/+}$ mice with CH-PH. Consequently, $Cx43^{+/-}$ mice with CH-PH were still alive and, although high, right ventricular systolic pressure and Fulton index were not higher than in $Cx43^{+/+}$ mice with CH-PH. Interestingly, in all groups of mice, heart rate and heart capillary density were similar and cardiomyocytes apoptosis was absent (figures S7c and S8). Therefore, blocking Cx43 functions or reducing Cx43 expression level should not worsen PH cardiac symptoms. Consistently, intratracheal instillation of ^{43}Gap26, a peptide that specifically inhibits Cx43, had a beneficial effect on LPS-induced lung inflammation in mice without any obvious deleterious side effects [32]. Importantly, Cx43 decrease in heart following PH has only been previously shown in monocrotaline PH model, that is considered to be closer to iPAH but not

in CH-PH models. Altogether, the present results strengthen the interest of targeting Cx43 in CH-PH.

We also addressed the role of Cx43 in PA vasoreactivity, another important feature that participates to PH development [33]. PA vasoreactivity was tested in response to ET-1 and 5-HT whose circulating concentrations are known to increase in PH [34-39]. PA vasoreactivity to ET-1 was increased in $Cx43^{+/-}$ compared to $Cx43^{+/+}$ in both N and CH conditions (figure 6a) whereas PA vasoreactivity to 5-HT was identical in all groups of mice (figure 6b). Such results are consistent with those observed by Htet et al. in $Cx43^{+/-}$ C57BL6 mice [11]. Such role of Cx43 on the PA vasoreactivity to ET-1 may explain why albeit PA remodelling and inflammation were absent, right ventricular systolic pressure and Fulton index remained high in $Cx43^{+/-}$ mice with CH-PH compared to $Cx43^{+/+}$ mice with CH-PH. Such ET-1-induced PA hyper-reactivity in $Cx43^{+/-}$ mice can be considered as a minor secondary effect since it could be treated with endothelin receptor antagonists that have already been shown to be of benefit for patients [1]. Collectively, these results indicate that Cx43 plays an important role in PA vasoreactivity under both physiological and pathophysiological conditions (N and CH-PH respectively) as already shown in the rat and C57BL6 mouse pulmonary circulation [7, 8, 11].

In conclusion, in the present study, we demonstrate, for the first time, that partial decrease of Cx43 expression suppresses PA remodelling and inflammation in mice with CH-PH. We also show that, even in the absence of pulmonary vascular remodelling, right ventricular pressures and hypertrophy remained high in $Cx43^{+/-}$ mice with CH-PH; importantly, we observe a slight reduction in cardiac hypertrophy suggesting that blocking Cx43 might have some beneficial effect on the heart. Since decrease in Cx43 expression also enhances PA vaoreactivity, we suggest that both Cx43 and ET-1 pathway inhibitors could be a new therapeutical option to further explore for PH. Finally, since Cx43 was increased in PA from patients with CH-PH

but not in patients with iPAH, we suggest that a treatment combining Cx43 and ET-1 blockers could be especially considered for patients with CH-PH.

Acknowledgements

The microscopy for TUNEL assay and labelling of Cx43, PCNA and vWF in mice lungs or heart sections was done in the Bordeaux Imaging Center, a service unit of the CNRS-INSERM and Bordeaux University, member of the national infrastructure France BioImaging. We thank Thierry Leste-Lasserre for his design of the primers at the Plateforme Transcriptome (Magendie Neurocenter in Bordeaux), a service unit of the CNRS-INSERM and Bordeaux University.

Conflict of interest

None.

Support statement: This study was granted by the Fondation du souffle and the Fonds de Dotation Recherche en Santé Respiratoire. B. Rode is funded by La Fondation Lefoulon Delalande.

References

1. Galie N, Humbert M, Vachiery JL, Gibbs S, Lang I, Torbicki A, Simonneau G, Peacock A, Vonk Noordegraaf A, Beghetti M, Ghofrani A, Gomez Sanchez MA, Hansmann G, Klepetko W, Lancellotti P, Matucci M, McDonagh T, Pierard LA, Trindade PT, Zompatori M, Hoeper M, Group ESCSD. 2015 ESC/ERS Guidelines for the diagnosis and treatment of pulmonary hypertension: The Joint Task Force for the Diagnosis and Treatment of Pulmonary Hypertension of the European Society of Cardiology (ESC) and the European Respiratory Society (ERS): Endorsed by: Association for European Paediatric and Congenital Cardiology (AEPC), International Society for Heart and Lung Transplantation (ISHLT). *Eur Heart J* 2016; 37: 67-119.
2. Guibert C, Marthan R, Savineau JP. Modulation of ion channels in pulmonary arterial hypertension. *Curr Pharm Des* 2007; 13: 2443-2455.
3. Humbert M, Lau EM, Montani D, Jais X, Sitbon O, Simonneau G. Advances in therapeutic interventions for patients with pulmonary arterial hypertension. *Circulation* 2014; 130: 2189-2208.
4. Rabinovitch M, Guignabert C, Humbert M, Nicolls MR. Inflammation and immunity in the pathogenesis of pulmonary arterial hypertension. *Circ Res* 2014; 115: 165-175.
5. Tamura Y, Phan C, Tu L, Le Hiress M, Thuillet R, Jutant EM, Fadel E, Savale L, Huertas A, Humbert M, Guignabert C. Ectopic upregulation of membrane-bound IL6R drives vascular remodeling in pulmonary arterial hypertension. *J Clin Invest* 2018; 128: 1956-1970.
6. Morrell NW, Adnot S, Archer SL, Dupuis J, Jones PL, MacLean MR, McMurtry IF, Stenmark KR, Thistlethwaite PA, Weissmann N, Yuan JX, Weir EK. Cellular and molecular basis of pulmonary arterial hypertension. *J Am Coll Cardiol* 2009; 54: S20-31.

7. Billaud M, Marthan R, Savineau JP, Guibert C. Vascular smooth muscle modulates endothelial control of vasoreactivity via reactive oxygen species production through myoendothelial communications. *PLoS One* 2009; 4: e6432.
8. Billaud M, Dahan D, Marthan R, Savineau JP, Guibert C. Role of the gap junctions in the contractile response to agonists in pulmonary artery from two rat models of pulmonary hypertension. *Respir Res* 2011; 12: 30.
9. Chen M, Liu Y, Yi D, Wei L, Li Y, Zhang L. Tanshinone IIA promotes pulmonary artery smooth muscle cell apoptosis in vitro by inhibiting the JAK2/STAT3 signaling pathway. *Cell Physiol Biochem* 2014; 33: 1130-1138.
10. Freund-Michel V, Muller B, Marthan R, Savineau JP, Guibert C. Expression and role of connexin-based gap junctions in pulmonary inflammatory diseases. *Pharmacol Ther* 2016; 164: 105-119.
11. Htet M, Nally JE, Shaw A, Foote BE, Martin PE, Dempsie Y. Connexin 43 Plays a Role in Pulmonary Vascular Reactivity in Mice. *Int J Mol Sci* 2018; 19.
12. Kim J, Hwangbo C, Hu X, Kang Y, Papangeli I, Mehrotra D, Park H, Ju H, McLean DL, Comhair SA, Erzurum SC, Chun HJ. Restoration of impaired endothelial myocyte enhancer factor 2 function rescues pulmonary arterial hypertension. *Circulation* 2015; 131: 190-199.
13. Yang L, Yin N, Hu L, Fan H, Yu D, Zhang W, Wang S, Feng Y, Fan C, Cao F, Mo X. Sildenefil increases connexin 40 in smooth muscle cells through activation of BMP pathways in pulmonary arterial hypertension. *Int J Clin Exp Pathol* 2014; 7: 4674-4684.
14. Yen CH, Tsai TH, Leu S, Chen YL, Chang LT, Chai HT, Chung SY, Chua S, Tsai CY, Chang HW, Ko SF, Sun CK, Yip HK. Sildenafil improves long-term effect of endothelial progenitor cell-based treatment for monocrotaline-induced rat pulmonary arterial hypertension. *Cytotherapy* 2013; 15: 209-223.

15. Brisset AC, Isakson BE, Kwak BR. Connexins in vascular physiology and pathology. *Antioxid Redox Signal* 2009; 11: 267-282.

16. Johnstone SR, Kroncke BM, Straub AC, Best AK, Dunn CA, Mitchell LA, Peskova Y, Nakamoto RK, Koval M, Lo CW, Lampe PD, Columbus L, Isakson BE. MAPK phosphorylation of connexin 43 promotes binding of cyclin E and smooth muscle cell proliferation. *Circ Res* 2012; 111: 201-211.

17. Liao Y, Regan CP, Manabe I, Owens GK, Day KH, Damon DN, Duling BR. Smooth muscle-targeted knockout of connexin43 enhances neointimal formation in response to vascular injury. *Arterioscler Thromb Vasc Biol* 2007; 27: 1037-1042.

18. Hardziyenka M, Campian ME, Verkerk AO, Surie S, van Ginneken AC, Hakim S, Linnenbank AC, de Bruin-Bon HA, Beekman L, van der Plas MN, Remme CA, van Veen TA, Bresser P, de Bakker JM, Tan HL. Electrophysiologic remodeling of the left ventricle in pressure overload-induced right ventricular failure. *J Am Coll Cardiol* 2012; 59: 2193-2202.

19. Sasano C, Honjo H, Takagishi Y, Uzzaman M, Emdad L, Shimizu A, Murata Y, Kamiya K, Kodama I. Internalization and dephosphorylation of connexin43 in hypertrophied right ventricles of rats with pulmonary hypertension. *Circ J* 2007; 71: 382-389.

20. Tanaka Y, Takase B, Yao T, Ishihara M. Right ventricular electrical remodeling and arrhythmogenic substrate in rat pulmonary hypertension. *Am J Respir Cell Mol Biol* 2013; 49: 426-436.

21. Freund-Michel V, Cardoso Dos Santos M, Guignabert C, Montani D, Phan C, Coste F, Tu L, Dubois M, Girerd B, Courtois A, Humbert M, Savineau JP, Marthan R, Muller B. Role of Nerve Growth Factor in Development and Persistence of Experimental Pulmonary Hypertension. *Am J Respir Crit Care Med* 2015; 192: 342-355.

22. Rodat-Despoix L, Aires V, Ducret T, Marthan R, Savineau JP, Rousseau E, Guibert C. Signalling pathways involved in the contractile response to 5-HT in the human pulmonary artery. *Eur Respir J* 2009; 34: 1338-1347.

23. Tu L, De Man FS, Girerd B, Huertas A, Chaumais MC, Lecerf F, Francois C, Perros F, Dorfmuller P, Fadel E, Montani D, Eddahibi S, Humbert M, Guignabert C. A critical role for p130Cas in the progression of pulmonary hypertension in humans and rodents. *Am J Respir Crit Care Med* 2012; 186: 666-676.

24. Parpaite T, Cardouat G, Mauroux M, Gillibert-Duplantier J, Robillard P, Quignard JF, Marthan R, Savineau JP, Ducret T. Effect of hypoxia on TRPV1 and TRPV4 channels in rat pulmonary arterial smooth muscle cells. *Pflugers Arch* 2016; 468: 111-130.

25. Reaume AG, de Sousa PA, Kulkarni S, Langille BL, Zhu D, Davies TC, Juneja SC, Kidder GM, Rossant J. Cardiac malformation in neonatal mice lacking connexin43. *Science* 1995; 267: 1831-1834.

26. Hara Y, Sassi Y, Guibert C, Gambaryan N, Dorfmuller P, Eddahibi S, Lompre AM, Humbert M, Hulot JS. Inhibition of MRP4 prevents and reverses pulmonary hypertension in mice. *J Clin Invest* 2011; 121: 2888-2897.

27. Tsang H, Leiper J, Hou Lao K, Dowsett L, Delahaye MW, Barnes G, Wharton J, Howard L, Iannone L, Lang NN, Wilkins MR, Wojciak-Stothard B. Role of asymmetric methylarginine and connexin 43 in the regulation of pulmonary endothelial function. *Pulm Circ* 2013; 3: 675-691.

28. Johnstone S, Isakson B, Locke D. Biological and biophysical properties of vascular connexin channels. *Int Rev Cell Mol Biol* 2009; 278: 69-118.

29. Cowan DB, Jones M, Garcia LM, Noria S, del Nido PJ, McGowan FX, Jr. Hypoxia and stretch regulate intercellular communication in vascular smooth muscle cells through reactive oxygen species formation. *Arterioscler Thromb Vasc Biol* 2003; 23: 1754-1760.

30. Tittarelli A, Janji B, Van Moer K, Noman MZ, Chouaib S. The Selective Degradation of Synaptic Connexin 43 Protein by Hypoxia-induced Autophagy Impairs Natural Killer Cell-mediated Tumor Cell Killing. *J Biol Chem* 2015; 290: 23670-23679.

31. Ahmed LA, Rizk SM, El-Maraghy SA. Pinocembrin ex vivo preconditioning improves the therapeutic efficacy of endothelial progenitor cells in monocrotaline-induced pulmonary hypertension in rats. *Biochem Pharmacol* 2017; 138: 193-204.

32. Sarieddine MZ, Scheckenbach KE, Foglia B, Maass K, Garcia I, Kwak BR, Chanson M. Connexin43 modulates neutrophil recruitment to the lung. *J Cell Mol Med* 2009; 13: 4560-4570.

33. Figueroa XF, Duling BR. Gap junctions in the control of vascular function. *Antioxid Redox Signal* 2009; 11: 251-266.

34. Carratu P, Scoditti C, Maniscalco M, Seccia TM, Di Gioia G, Gadaleta F, Cardone RA, Dragonieri S, Pierucci P, Spanevello A, Resta O. Exhaled and arterial levels of endothelin-1 are increased and correlate with pulmonary systolic pressure in COPD with pulmonary hypertension. *BMC Pulm Med* 2008; 8: 20.

35. Eddahibi S, Guignabert C, Barlier-Mur AM, Dewachter L, Fadel E, Dartevelle P, Humbert M, Simonneau G, Hanoun N, Saurini F, Hamon M, Adnot S. Cross talk between endothelial and smooth muscle cells in pulmonary hypertension: critical role for serotonin-induced smooth muscle hyperplasia. *Circulation* 2006; 113: 1857-1864.

36. Giaid A, Yanagisawa M, Langleben D, Michel RP, Levy R, Shennib H, Kimura S, Masaki T, Duguid WP, Stewart DJ. Expression of endothelin-1 in the lungs of patients with pulmonary hypertension. *N Engl J Med* 1993; 328: 1732-1739.

37. Kereveur A, Callebert J, Humbert M, Herve P, Simonneau G, Launay JM, Drouet L. High plasma serotonin levels in primary pulmonary hypertension. Effect of long-term epoprostenol (prostacyclin) therapy. *Arterioscler Thromb Vasc Biol* 2000; 20: 2233-2239.

38. Kim FY, Barnes EA, Ying L, Chen C, Lee L, Alvira CM, Cornfield DN. Pulmonary artery smooth muscle cell endothelin-1 expression modulates the pulmonary vascular response to chronic hypoxia. *Am J Physiol Lung Cell Mol Physiol* 2015; 308: L368-377.

39. Stewart DJ, Levy RD, Cernacek P, Langleben D. Increased plasma endothelin-1 in pulmonary hypertension: marker or mediator of disease? *Ann Intern Med* 1991; 114: 464-469.

Figure 1. Expression of Cx43 in human PH. (a) Expression of Cx43 assessed by Western Blot analysis in PA from patients with CH-PH (black column) compared with control patients (white column). (b and c) Expression of Cx43 assessed by Western Blot analysis in, respectively, PA-SMC and pulmonary microvascular endothelial cells (PM-ECs) from patients with iPAH (grey column) compared with control patients (white column). Cx43 expression was normalized to calnexin (a) or β-actin (b and c). Data represent means ± SEM. **P*<0.05. n is the number of patients.

Figure 2. Localization and expression of Cx43 in human PH. Expression and localization of Cx43 assessed by immunofluorescent staining in sections of intrapulmonary arteries from lungs of patients with CH-PH or iPAH compared with control patients. Cx43 is labelled in red, PA media is labelled with an antibody against α-smooth muscle actin (α-SMA) in white, endothelium is labelled with a lectin in green and nuclei are labelled with DAPI in blue. L is the PA lumen. Scale bar is 20 μm.

Figure 3. Localization and expression of Cx43 in intrapulmonary arteries from mice with CH-PH. Cx43 mRNA and protein levels were assessed by quantitative PCR and Western Blot analysis (a and b respectively) in $Cx43^{+/-}$ mice compared with $Cx43^{+/+}$ mice in N and CH conditions. Cx43 protein expression was normalized to GAPDH. Data represent means ± SEM. **P*<0.05, ***P*<0.01 and ****P*<0.001. n is the number of mice. c shows expression and localization of Cx43 protein assessed by immunofluorescent staining in sections of intrapulmonary arteries from lungs of $Cx43^{+/-}$ mice compared with $Cx43^{+/+}$ mice in N and CH conditions. Cx43 is labelled in red, nuclei are labelled with DAPI in blue and green is the elastic lamina autofluorescence. L is the PA lumen. Scale bar is 10 μm.

Figure 4. Remodelling of intrapulmonary arteries and right ventricle in hypoxia-induced PH in mice. (a) Representative sections of intrapulmonary arteries (haematoxylin and eosin staining) from lungs of $Cx43^{+/-}$ mice compared with $Cx43^{+/+}$ mice in N and CH conditions. Scale bar is 15 µm. (b) Percentage of the intrapulmonary arterial wall thickness in the different experimental groups as shown in a. White and black columns represent N and CH conditions respectively. PCNA (proliferating cell nuclear antigen) expression was assessed by immunofluorescent staining (c) and TUNEL-methodology was used to detect apoptotic cells (e) in intrapulmonary arteries from lungs sections of $Cx43^{+/-}$ mice compared with $Cx43^{+/+}$ mice in N and CH conditions (white and black columns respectively). Mouse colon was used as a positive control (right picture in e). Nuclei of proliferating or apoptotic cells were labelled in red (c and e respectively). Nuclei of all cells are labelled with DAPI in blue and green is autofluorescence of the elastic lamina. L is the PA lumen. Scale bar is 50 µm (c and e). d is the percentage of PCNA positive cells in the different experimental groups of mice as shown in c. f shows right ventricular systolic pressure recordings and g shows right ventricular remodelling (assessed by the Fulton index) in $Cx43^{+/-}$ mice compared with $Cx43^{+/+}$ mice in N and CH conditions (white and black columns respectively). n is the number of vessels from 4-5 mice per group for b and d and number of mice for f and g. Data represent means ± SEM (b, d, f, g). $*P<0.05$, $**P<0.01$ and $***P<0.001$.

Figure 5. Lung inflammation in $Cx43^{+/-}$ mice compared with $Cx43^{+/+}$ mice in N and CH conditions. CD45 (a leukocyte marker) expression was assessed by Western Blot analysis in whole lung homogenates (a) and by immunofluorescent labelling in lung sections (red labelling in b) from $Cx43^{+/-}$ mice compared with $Cx43^{+/+}$ mice in N and CH conditions (white

and black columns respectively). For Western Blotting experiments, CD45 expression was normalized to GAPDH and expressed as a percentage of the CD45 expression in lungs from $Cx43^{+/+}$ mice in N conditions (a). Nuclei were labelled with DAPI in blue (b). b1, b2, b3, b4, b5, b6, b7 and b8 are zooms from the similarly identified squares on the respective above pictures. Scale bar is 100 µm. Data represent means ± SEM in a. n is the number of mice. ***P<0.001.

Figure 6. Pulmonary arterial reactivity in $Cx43^{+/-}$ mice compared with $Cx43^{+/+}$ mice in N and CH conditions. Contraction of intrapulmonary arterial rings was induced by cumulative concentrations of either endothelin-1 (ET-1; 0.1 to 100 nM; a), serotonin (5-HT; 0.001 to 10 µM; b) or phenylephrine (Phe; 0.001 to 30 µM; c) in $Cx43^{+/-}$ mice (white symbols) compared with $Cx43^{+/+}$ mice (black symbols) in N and CH (left and right graphs respectively). Relaxation of intrapulmonary arterial rings was induced by cumulative concentrations of carbachol (Carb; 0.01 to 1000 µM, d) on vessels pre-contracted with Phe 1 µM in $Cx43^{+/-}$ mice (white symbols) compared with $Cx43^{+/+}$ mice (black symbols) in N and CH (left and right graphs respectively). Data represent means ± SEM. n is the number of vessels from at least 3 mice per condition. e shows endothelium labelling with von Willebrand Factor (vWF) in red in $Cx43^{+/-}$ mice compared with $Cx43^{+/+}$ mice in N and CH conditions. Nuclei are labelled with DAPI in blue. Scale bar is 20 µm. *P<0.05 and **P<0.01.

Figure 7. Expression and localization of Cx43 in right *versus* left heart ventricles from $Cx43^{+/-}$ mice compared with $Cx43^{+/+}$ mice in N and CH conditions. Cx43 mRNA (a and b) and protein (c and d) levels were assessed by quantitative PCR and Western Blot analysis in right *versus* left heart ventricles from $Cx43^{+/-}$ mice compared with $Cx43^{+/+}$ mice in N and CH

(white and black columns respectively). Cx43 protein expression was normalized to GAPDH. Data represent means ± SEM (a, b, c and d). *P<0.05, **P<0.01 and ***P<0.001. n is the number of mice. (e) Localization of Cx43 protein assessed by immunofluorescent staining in sections of right or left heart ventricles (top and bottom pictures respectively) from $Cx43^{+/-}$ mice compared with $Cx43^{+/+}$ mice in N and CH conditions. Scale bar is 100 µm. Cx43 labelling is red and nuclei are labelled with DAPI in blue.

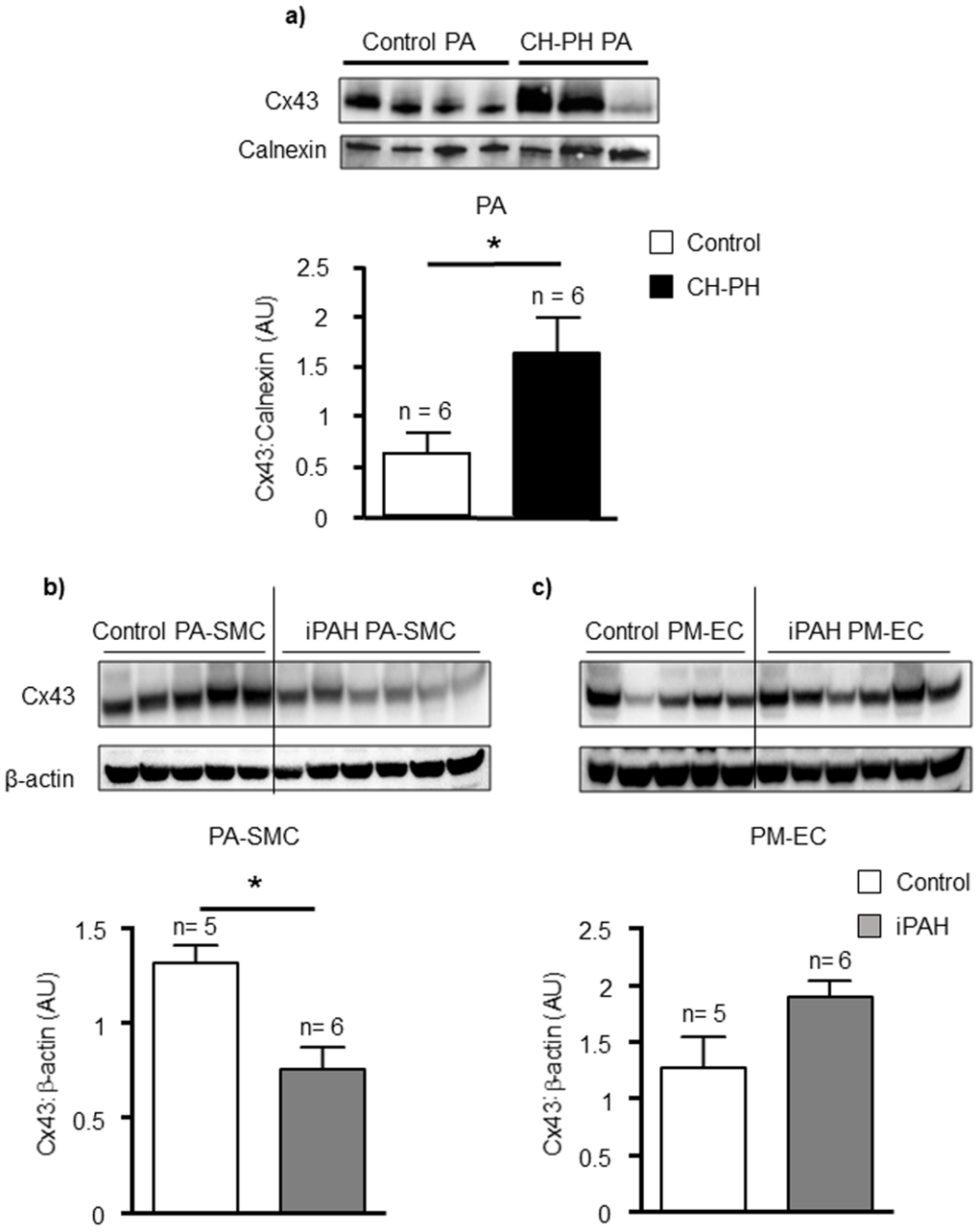
a)
Control PA
CH-PH PA
Cx43
Calnexin
PA
*
Control
CH-PH
Cx43:Calnexin (AU)
2.5
2
1.5
1
0.5
0
n = 6
n = 6
b)
Control PA-SMC
iPAH PA-SMC
Cx43
β-actin
PA-SMC
*
Cx43: β-actin (AU)
1.5
1
0.5
0
n= 5
n= 6
c)
Control PM-EC
iPAH PM-EC
PM-EC
Control
iPAH
Cx43: β-actin (AU)
2.5
2
1.5
1
0.5
0
n= 5
n= 6

FIGURE 1

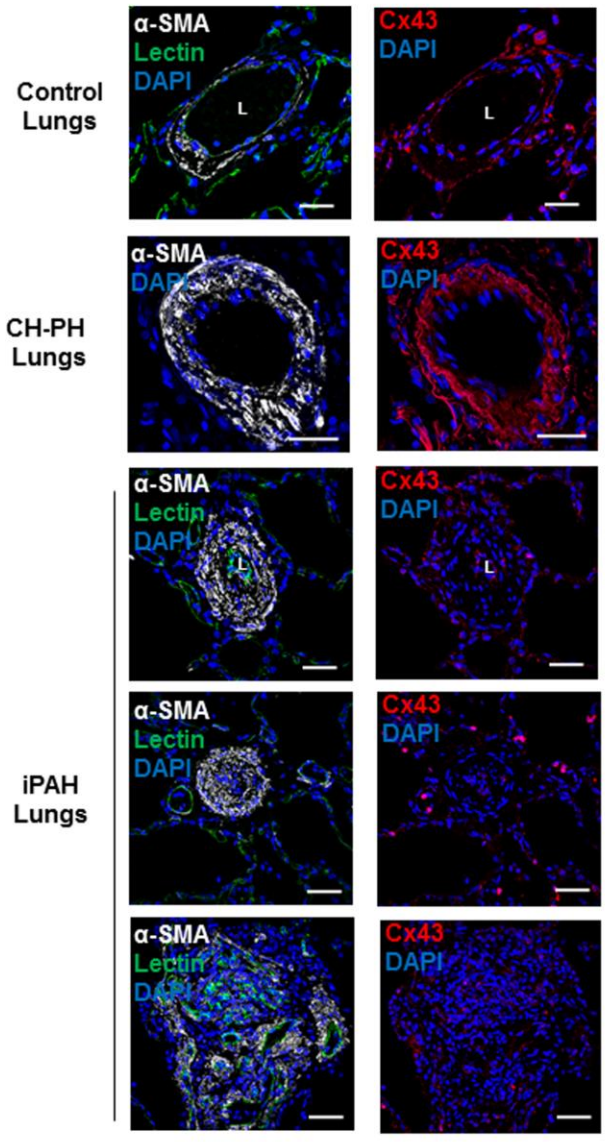
Control Lungs
CH-PH Lungs
iPAH Lungs
α-SMA
Lectin
DAPI
Cx43
DAPI
L

FIGURE 2

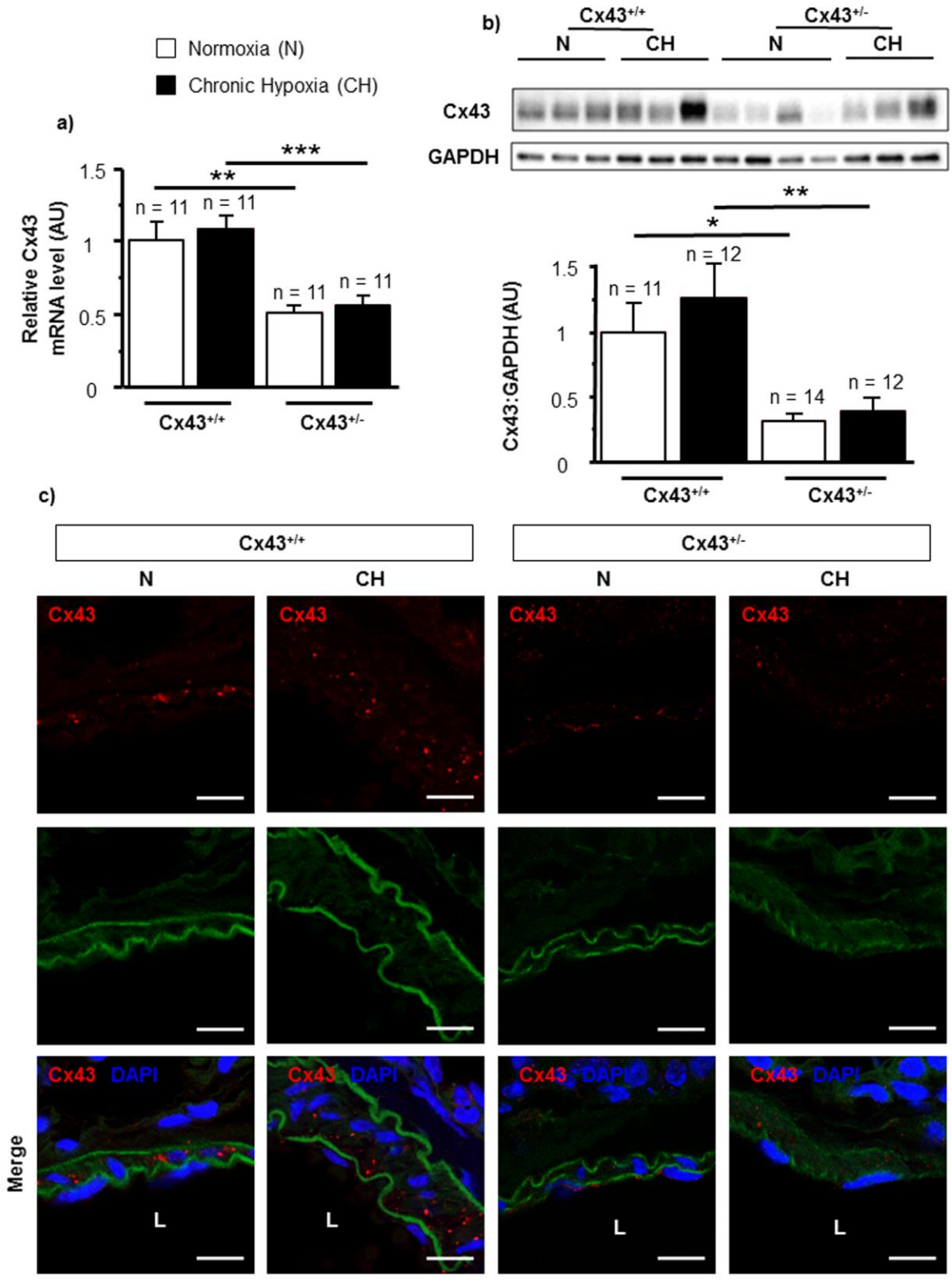
a)
Normoxia (N)
Chronic Hypoxia (CH)
Relative Cx43 mRNA level (AU)
1.5
1
0.5
0
n = 11
n = 11
n = 11
n = 11
**
***
Cx43+/+
Cx43+/-
b)
Cx43+/+
Cx43+/-
N
CH
N
CH
Cx43
GAPDH
**
*
Cx43:GAPDH (AU)
1.5
1
0.5
0
n = 11
n = 12
n = 14
n = 12
Cx43+/+
Cx43+/-
c)
Cx43+/+
Cx43+/-
N
CH
N
CH
Cx43
Cx43
Cx43
Cx43
Cx43 DAPI
Cx43 DAPI
Cx43 DAPI
Cx43 DAPI
Merge
L
L
L
L

FIGURE 3

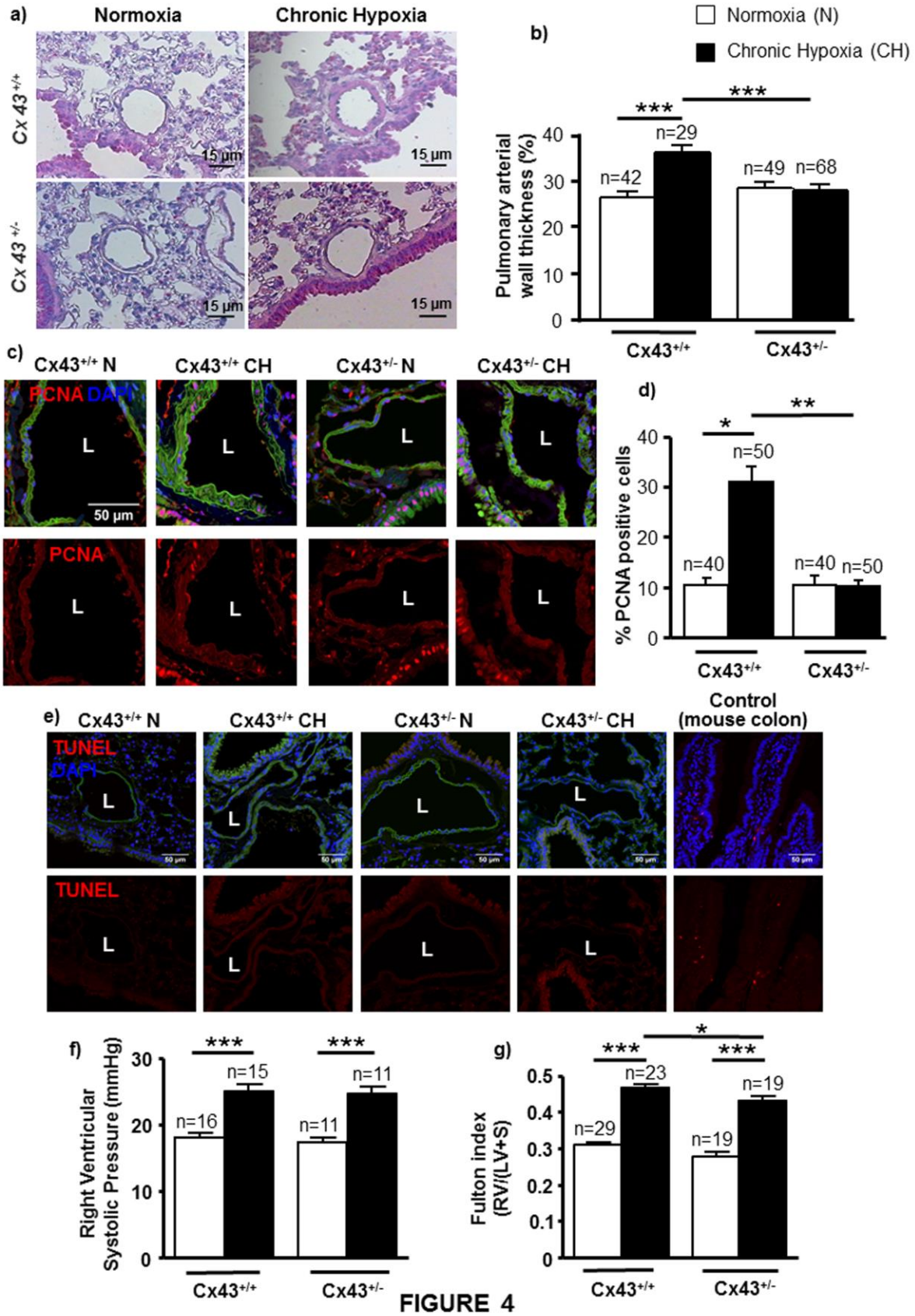
a)
Normoxia
Chronic Hypoxia
Cx 43+/+
Cx 43+/-
15 µm
b)
Normoxia (N)
Chronic Hypoxia (CH)
Pulmonary arterial wall thickness (%)
***
***
n=42
n=29
n=49
n=68
Cx43+/+
Cx43+/-
c)
Cx43+/+ N
Cx43+/+ CH
Cx43+/- N
Cx43+/- CH
PCNA DAPI
PCNA
L
50 µm
d)
% PCNA positive cells
*
**
n=40
n=50
n=40
n=50
e)
Cx43+/+ N
Cx43+/+ CH
Cx43+/- N
Cx43+/- CH
Control (mouse colon)
TUNEL
DAPI
f)
Right Ventricular Systolic Pressure (mmHg)
n=16
n=15
n=11
n=11
g)
Fulton index (RV/(LV+S))
n=29
n=23
n=19
n=19

FIGURE 4

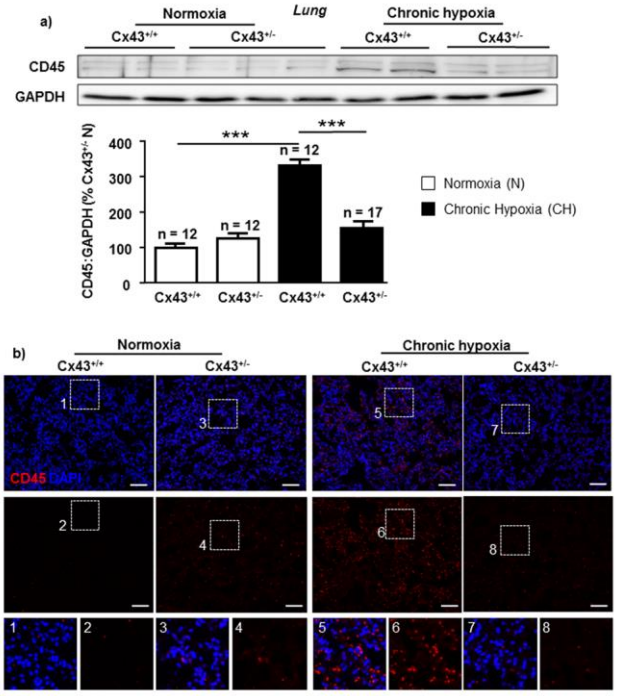
a)
Normoxia
Lung
Chronic hypoxia
Cx43+/+
Cx43+/-
Cx43+/+
Cx43+/-
CD45
GAPDH
CD45:GAPDH (% Cx43+/- N)
400
300
200
100
0
***
***
n = 12
n = 12
n = 12
n = 17
Cx43+/+
Cx43+/-
Cx43+/+
Cx43+/-
Normoxia (N)
Chronic Hypoxia (CH)
b)
Normoxia
Chronic hypoxia
Cx43+/+
Cx43+/-
Cx43+/+
Cx43+/-
CD45 DAPI
1
2
3
4
5
6
7
8

FIGURE 5

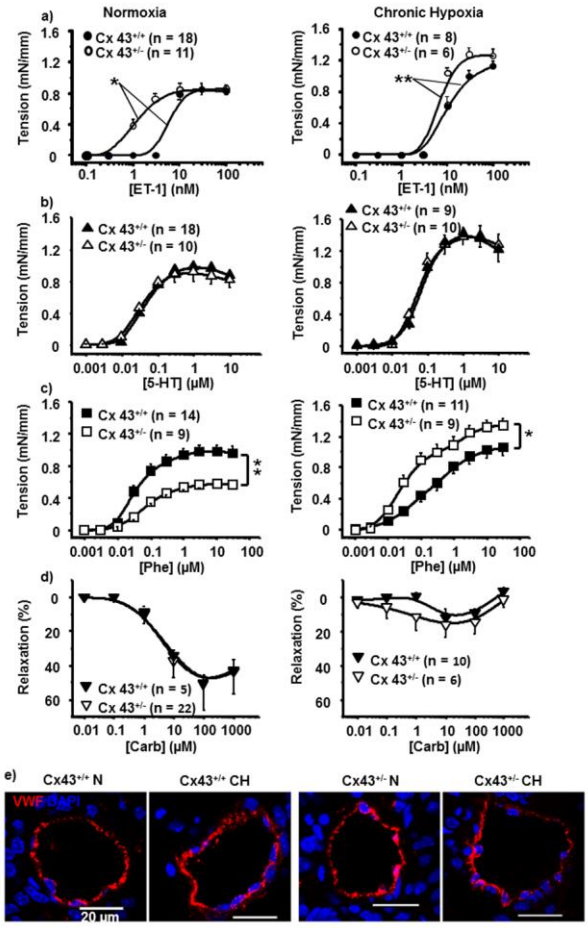
a)
Normoxia
Chronic Hypoxia
Cx 43+/+ (n = 18)
Cx 43+/- (n = 11)
Cx 43+/+ (n = 8)
Cx 43+/- (n = 6)
Tension (mN/mm)
[ET-1] (nM)
b)
Cx 43+/+ (n = 18)
Cx 43+/- (n = 10)
Cx 43+/+ (n = 9)
Cx 43+/- (n = 10)
[5-HT] (μM)
c)
Cx 43+/+ (n = 14)
Cx 43+/- (n = 9)
Cx 43+/+ (n = 11)
Cx 43+/- (n = 9)
[Phe] (μM)
d)
Relaxation (%)
Cx 43+/+ (n = 5)
Cx 43+/- (n = 22)
Cx 43+/+ (n = 10)
Cx 43+/- (n = 6)
[Carb] (μM)
e)
Cx43+/+ N
Cx43+/+ CH
Cx43+/- N
Cx43+/- CH
VWF DAPI
20 μm

FIGURE 6

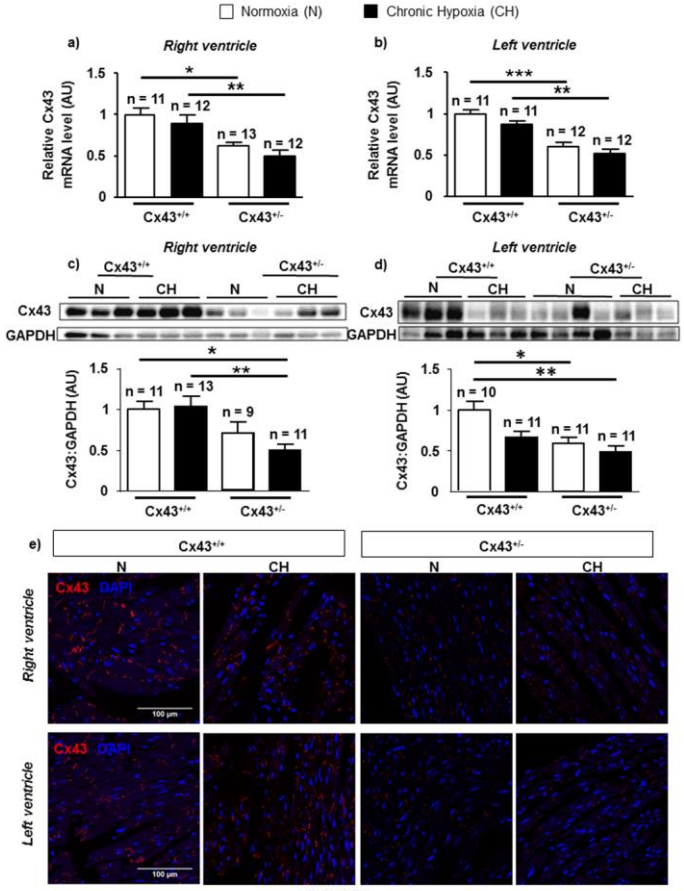
Normoxia (N)
Chronic Hypoxia (CH)
a)
Right ventricle
Relative Cx43 mRNA level (AU)
b)
Left ventricle
c)
Right ventricle
d)
Left ventricle
Cx43
GAPDH
Cx43:GAPDH (AU)
e)
Cx43+/+
Cx43+/-
N
CH
Right ventricle
Left ventricle
Cx43 DAPI
100 µm

FIGURE 7

Online data supplement

Connexin 43 Is a Promising Target for Pulmonary Hypertension due To Hypoxemic Lung Disease

Claire Bouvard, Nafiisha Genet, Carole Phan, Baptiste Rode, Raphaël Thuillet, Ly Tu, Paul Robillard, Marilyne Campagnac, Raffaella Soleti, Eric Dumas De La Roque, Frédéric Delcambre, Laurent Cronier, Thibaud Parpaite, Elise Maurat, Patrick Berger, Jean-Pierre Savineau, Roger Marthan, Christophe Guignabert, Véronique Freund-Michel, Christelle Guibert

Detailed Methods

Human pulmonary arterial cell cultures

Human pulmonary smooth muscle cells (PA-SMC) were obtained and cultured as previously described [1, 2]. Human pulmonary arteries were initially cut into several pieces (1–2 mm^2) and placed at the bottom of individual wells of six-well culture plates containing culture medium (DMEM–HEPES supplemented with 1% penicillin–streptomycin and 1% nonessential amino acids) enriched with 10% foetal calf serum. PA-SMC were then isolated with trypsin-EDTA and cultured in 75 cm^2 flasks (Costar) in a humidified chamber at 37°C (5 % CO_2), with the medium changed twice a week. Cells were characterized as smooth muscle cells both morphologically (typical "hills and valleys" morphology) and immunocytochemically using antibodies directed against calponin 1/2/3 and α-smooth muscle actin (Sigma-Aldrich). Immunostaining demonstrated the presence of a population of smooth muscle cells with approximately 95% purity. Cells were used experimentally at passage 3 to 6. All cell culture products were purchased from Invitrogen.

PA-SMC exposure to chronic hypoxia *in vitro* was performed as previously described [3]. PA-SMC in the control group (“Normoxia” - N) were exposed to a gas mixture containing 21 % O_2, 74 % N_2, and 5 % CO_2. Cells in the chronic hypoxia group (CH) were exposed to a gas mixture containing 1 % O_2, 94 % N_2, and 5 % CO_2 for 24 or 48 h in a tri-gas incubator (Heracell 150i, ThermoScientific, Saint Herblain, France).

Animal experiments

All animal studies conformed to the Declaration of Helsinki conventions for the use and care of animals. Agreement (number A33-063-907) was obtained from the French authorities and

all the protocols used were approved by the local ethics committee (Comité d'éthique de Bordeaux n° 50, protocol number APAFIS#9212-2017031018562273 v5). Genetically modified adult male CD1 mice (8 – 12 weeks) ($Gja1^{tm1Kdr}$; Jackson Laboratory, Bar Harbor, ME) were used and compared to their origin's strain mice. Mutation is due to the in-frame insertion of a promoterless neomycin (Neo) gene into exon 2 of Cx43 (Gja1) gene [4]. $Gja1^{tm1Kdr}$ homozygous ($Cx43^{-/-}$) mice die at birth due to a severe heart defect [4]. Consequently, only heterozygous ($Cx43^{+/-}$) and wild-type ($Cx43^{+/+}$) mice were used for the study. Tails from such mice were used for genotyping as previously described [5]. PH was induced by exposing mice to chronic hypoxia (CH) in a hypobaric chamber (380 mmHg) during 21 days while control animals were kept under normobaric normoxia (N - room air). Chambers were opened three times a week for animal care and cleaning, and all animals had free access to food and water.

Hemodynamic measurements and assessment of right ventricular hypertrophy

Mean pulmonary arterial pressures (mPAP) were measured in mice as previously described [6]. Mice were anesthetized with an intraperitoneal injection of Exagon® (50 mg/kg of body weight, Centravet) and after thoracotomy, a heparin-filled hypodermic needle connected to a polyethylene catheter was placed into the right ventricular cavity by direct puncture of the right ventricle. Right ventricular systolic pressure was measured by use of a fluid-filled force transducer. The Fulton index or weight ratio: right ventricle (RV) / (left ventricle (LV) + septum (S)) was calculated to assess hypoxia-induced right ventricular hypertrophy.

Hemodynamic responses to carbachol

Mice were anesthetized with an intraperitoneal injection of Exagon® (50 mg/kg of body weight, Centravet). A tracheotomy was performed and animals were ventilated with a small-animal ventilator (Minivent type 845, Hugo Sachs Elektronik, Germany). Body temperature was maintained with a heating platform. Bosentan and carbachol were administered via a catheter in the jugular vein and right ventricular systolic pressure was measured as described in the previous section. We blocked the endothelin A and B receptors with the antagonist bosentan administered at 20 mg/kg and 5 minutes later, we administered the vasodilator carbachol at 10 µM. Right ventricular systolic pressure was recorded just before carbachol injection and up to five minutes after carbachol injection. The carbachol effect measured, was the maximal effect observed during the five minutes of recordings.

Measurement of right ventricular function by echocardiography

Anesthesia of mice was induced with isoflurane gas (3 %) and maintained with 1.5 % isoflurane in room air supplemented with 100 % O_2. Mice were laid in supine position on a heating platform with all legs taped. The chest of mice was shaved. To provide a coupling medium for the transducer, a pre-warmed ultrasound gel was spread over the chest wall. Transthoracic echocardiography was performed with the Vevo770 high-resolution imaging system equipped with a 40-MHz transducer (RMV 704). Pulsed-wave Doppler was used to measure pulmonary artery flow through the pulmonary valve. Pulmonary artery acceleration time (PAAT) and velocity-time integral (VTI) were recorded.

Measurement of pulmonary arterial reactivity

After mice euthanasia by cervical dislocation, a thoracotomy was performed, and after exsanguination, the left lung was rapidly removed and rinsed in Krebs solution containing 119 mM NaCl, 4.7 mM KCl, 1.5 mM $CaCl_2$, 25 mM $NaHCO_3$, 1.2 mM KH_2PO_4 and 5 mM glucose. Intrapulmonary arteries were dissected free from surrounding connective tissues under binocular control, and arterial segments were mounted in a Mulvany myograph (Multi Myograph System, model 610M, J.P. trading) as previously described [7]. Arterial viability was assessed using physiological salt solution containing 80 mM KCl (equimolar substitution with NaCl). Contractile responses were obtained by constructing a cumulative concentration-response curve to endothelin-1 (ET-1; 0.1 to 100 nM), serotonin (5-HT; 0.001 to 10 µM) or phenylephrine (Phe; 0.001 to 30 µM). Relaxation was assessed by applying cumulative concentrations of carbachol (Carb; 0.01 to 1000 µM) on vessels pre-contracted with Phe 1 µM.

Measurements of pulmonary arterial medial wall thickness

Mice lungs were fixed in 4% paraformaldehyde, and dehydrated in increasing grade of ethanol. After delipidation with xylene, lungs were embedded in paraffin and cut into transverse sections (4 µm) which were stained with haematoxylin and eosin. Pulmonary vascular remodelling was assessed by measuring the percentage of wall thickness of the intra-acinar arteries with an external diameter of less than 80 µm (74.2 ± 4 µm). 3 to 10 vessels per mice were analysed in a blinded fashion using Image J software (NIH Image). The percentage of wall thickness (% wall thickness) was calculated as [(external wall areas) – (internal wall areas)] x 100/ external wall areas.

Immunofluorescent staining

Serial 4 µm mice lung or heart sections or 5 µm human lung sections were deparaffinised and rehydrated. For antigen retrieval, sections were either heated at 95°C for 20 minutes in citrate buffer (pH 6) for proliferative cell nuclear antigen (PCNA) immunostaining or incubated in pronase E 0.1 % (Sigma-Aldrich) for Cx43, von Willebrand factor (vWF), CD31 immunostainings or incubated in a retrieval buffer for immunostaining of CD45 (a pan leukocyte marker) in mice lung and/or heart sections and alpha-smooth muscle actin (α-SMA), lectin, Cx37, Cx40 and Cx43 in human lung sections. Unspecific protein binding was blocked with a blocking buffer composed of bovine serum albumin (BSA 5%) and goat serum (5 %) (Sigma-Aldrich) for PCNA, Cx43, vWF and CD31 in mice lung and/or heart sections and then incubated overnight at 4°C with specific primary antibodies followed by incubation with corresponding secondary fluorescent-labelled antibodies (Thermo Fisher Scientific). Details on the primary and secondary antibodies are shown in the supplemental table S1. Nuclei were stained with DAPI (Sigma-Aldrich). Plasma membranes were stained with WGA-FITC (W834, Invitrogen). Negative controls were performed in parallel by omitting primary antibodies. The percentage of PCNA positive cells in intrapulmonary arteries was assessed in five to ten vessels (with a mean diameter of 70 µm) per section. In addition, TUNEL assay was performed using the ApopTag® Red In Situ Apoptosis Detection Kit (S7165, Merck), according to the manufacturer's protocol. Mounting was performed using ProLong Gold antifade reagent (Thermo Fischer Scientific) or Dako fluorescence mounting medium (Agilent). Images were taken using an LSM700 confocal microscope (Zeiss) for human lung sections and CD45 labelling in mice lung sections, using a LSM880 Airyscan confocal microscope (Zeiss) for mouse lung CX43/WGA labelling and for all other fluorescent labellings a TCS SP8 confocal microscope (Leica) was used.

Western Blot analysis

Intrapulmonary arteries, left or right ventricles from mice of the different experimental groups were homogenized in RIPA buffer containing 1 % triton X-100 and protease and phosphatase inhibitors (Sigma-Aldrich). Human PA-SMC and PM-EC were homogenized and sonicated in RIPA buffer containing protease and phosphatase inhibitors (Sigma-Aldrich). CD45 expression was performed on mice whole lung homogenates. Whole lung samples were homogenized in ice-cold lysis buffer containing 50 mM Tris-HCl pH 7.4, 1 % NP-40, 0.25 % sodium deoxycholate, 150 mM NaCl, 1 mM EDTA, 1 mM NaF, 1 mM PMSF and protease and phosphatase inhibitors (Sigma-Aldrich). For all the Western Blotting experiments, the protein concentration was determined by using the Lowry method (Bio-Rad). Equal amounts of proteins (50 µg for human PA-SMC and PM-EC, 30 µg for human pulmonary arteries, 15 µg for mice intrapulmonary arteries, 25 µg for mice whole lung homogenates and 30 µg for mice right and left ventricles), were separated by SDS-PAGE and transferred to a nitrocellulose membrane. After blocking, membranes were incubated overnight at 4°C with one of the specific primary antibodies (details on primary antibodies are shown in the supplemental table S1). Antibodies against β-actin, calnexin and GAPDH were used as loading controls. Membranes were then incubated with corresponding horseradish peroxidase-conjugated secondary antibodies. Immunoreactive proteins were detected by chemiluminescence with an ECL detection system (Substrate HRP Immobilon Western, Millipore). ChemiDoc XRS+ system (Biorad) was used for blot imaging and Image Lab software (Biorad) was used for analysis.

Quantitative real-time PCR

Total RNA of intrapulmonary arteries, right and left ventricles from mice was isolated by using the RNeasy plus micro kit (Qiagen) according to the manufacturer's instructions. Total RNA of human PA-SMC was isolated by using the Nucleospin RNA plus kit (Macherey Nagel) according to the manufacturer's instructions. cDNA of 1 µg ARN for human cells and 150 ng ARN for mice tissues were reverse-transcribed by using the qScript cDNA supermix reverse transcription kit (Quantabio). After reverse transcription, PCR was performed on the CFX Connect thermocycler (Biorad). 5 ng ADNc was amplified in duplicate by 40 cycles of 10 s at 95°C, 30 s at Tm 60°C for all primers (see table S2 for details on primers) using PerfeCTa SYBR Green supermix (Quantabio) and gene specific primers for Cx37, Cx40 and Cx43 (table S2 for details). The mRNA expression level of these genes of interest was determined using the comparative $2^{-\Delta\Delta Ct}$ method and normalized to the mRNA expression level of endogenous references by using geometric averages of 3 or 4 internal housekeeping genes (i.e. SDHA, GUSB, RPLPO and GAPDH for mice samples and GAPDH, HPRT1 and RPLPO for human samples – details on primers for housekeeping genes are shown in table S2) and according to Normfinder software [8].

Supplemental table S1

Protein	Source	Reference	Reactivity	Application	Dilution
α-SMA	Santa Cruz	Sc-32251	Mice – Rat - Human	Immunostaining	1:100
β-actin	Sigma-Aldrich	A3854	Human	Western Blot	1:5000
Calnexin	Santa Cruz	Sc-11397	Human	Western Blot	1:1000
CD45	Santa Cruz	SC-25590	Mice	Western Blot	1:200
CD45	Biotechne	BAM114	Mice	Immunostaining	1:50
CD31	Abcam	Ab24590	Mice – rat - human	Immunostaining	1:200
Connexin 37	Invitrogen	404300	Human	Immunostaining	1:200
Connexin 40	Tebu	Sc-20466	Human	Immunostaining	1:200
Connexin 43	Sigma-Aldrich	C6219	Human	Western Blot, immunostaining	1:400
Connexin 43	Sigma-Aldrich	C6219	Mice	Western Blot, immunostaining	1:2000 for immunostaining and 1:5000 for Western Blot
GAPDH	Santa Cruz	FL-335	Mice	Western Blot	1:1000
Lectin	Sigma	L8262	Human	Immunostaining	1:500
PCNA	Abcam	Ab29	Mice	Immunostaining	1:5000
von Willebrand Factor	Millipore	AB7356	Mice	Immunostaining	1:100

Supplemental table S2

Gene	Species	Genebank accession number	Sequence	Product size (bp)
mGja1 (Cx43)	mouse	NM_010288.3	CATCAGGGAGGCAAGCCAT TTACACACTTGCACACCCACAC	71
mGja4 (Cx37)	mouse	NM_008120.3	CTTACCCCAACCTCACCCTATG TCCTGTGAGGAGAGGGTTTGA	70
mGja5 (Cx40)	mouse	NM_001271628.1	TCTGACTCACCTGCCCATCTC CTCATTTATCTTTCCACCCAACAA	73
mGUSB	mouse	NM_010368.2	GAAGGCTGGCTCACAATTTAAGA GGTGGGTGCTAGGAATTGAATC	71
mSDHA	mouse	NM_023281.1	TACAAAGTGCGGGTCGATGA TGTTCCCCAAACGGCTTCT	74
mRPLPO	mouse	NM_007475.5	CTGAACATCTCCCCCTTCTCC GGGTTATAAATGCTGCCGTTGT	71
mGAPDH	mouse	NM_001289726.1	GCCAAAAGGGTCATCATCTCCG ATGAGCCCTTCCACAATGCC	179
hGJA1 (Cx43)	human	NM_000165.3	CGGGAAGCACCATCTCTAACT CGCTGGTCCACAATGGCTAGT	118
hGAPDH	human	NM_002046.6	CACATGGCCTCCAAGGAGTAA TGAGGGTCTCTCTCTTCCTCTTGT	75
hHPRT1	human	NM_000194.2	GGCAGTATAATCCAAAGATGGTCAA TCAAGGGCATATCCTACAACAAAC	130
hRPLP0	human	NM_001002.3	TCGTGGAAGTGACATCGTCTTT CTGTCTTCCCTGGGCATCA	74

Supplemental Figure Legends

Figure S1. Localization and expression of Cx43 in human PH. Expression and localization of Cx43 were assessed by immunofluorescent staining in sections of intrapulmonary arteries from lungs of patients with CH-PH or iPAH compared with control patients. Cx43 is labelled in red, PA media is labelled with an antibody against α-smooth muscle actin (α-SMA) in white, endothelium is labelled with a lectin in green and nuclei are labelled with DAPI in blue. L is the PA lumen. Scale bar is 20 μm.

Figure S2. Effect of CH on Cx43 mRNA expression in human PA-SMC. Histogram shows Cx43 mRNA in PA-SMC from control patients in N (white columns) versus CH (1 % O_2 – black columns) during 24 h or 48 h. Data represent means ± SEM. $^{**}P<0.01$ and $^{***}P<0.001$. n is the number of patients.

Figure S3. Localization and expression of Cx37 and 40 in human PH. Expression and localization of Cx37 and 40 were assessed by immunofluorescent staining in sections of intrapulmonary arteries from lungs of patients with iPAH or CH-PH compared with control patients. Cx37 or 40 is labelled in red, PA media is labelled with an antibody against α-smooth muscle actin (α-SMA) in white, endothelium is labelled with an antibody against lectin in green and nuclei are labelled with DAPI in blue. L is the PA lumen. Scale bar is 20 μm.

Figure S4. Localization of Cx43 in the intrapulmonary arteries from mice with CH-PH. Expression of Cx43 protein was assessed by immunofluorescent staining and confocal

microscopy with high magnification in sections of intrapulmonary arteries from lungs of $Cx43^{+/-}$ mice compared with $Cx43^{+/+}$ mice in N and CH conditions. Cx43 is labelled in red, nuclei are labelled with DAPI in blue and membrane is labelled with WGA-FITC in green. Right pictures are merge of their respective left pictures. Scale bar is 10 µm.

Figure S5. Localization and expression of Cx43 in intrapulmonary arteries from mice with CH-PH. Expression and localization of Cx43 protein were assessed by immunofluorescent staining in sections of intrapulmonary arteries from lungs of $Cx43^{+/-}$ mice compared with $Cx43^{+/+}$ mice in N and CH conditions. Cx43 is labelled in red, nuclei are labelled with DAPI in blue and green is the elastic lamina autofluorescence. White arrows show the red punctate labelling of Cx43. L is the PA lumen. Scale bar is 100 µm in the top pictures and 10 µm in all the other pictures which are zoom of their respective top pictures.

Figure S6. Expression of Cx37 and 40 mRNA in pulmonary arteries from $Cx43^{+/-}$ mice compared with $Cx43^{+/+}$ mice in N and CH (white and black columns respectively). mRNAs were assessed by quantitative PCR for Cx37 in a and Cx40 in b. Data represent means ± SEM. n is the number of mice.

Figure S7. Right ventricular function in $Cx43^{+/-}$ mice compared with $Cx43^{+/+}$ mice in N and CH conditions. (a) representative pulmonary artery flow through the pulmonary valve from $Cx43^{+/-}$ mice compared with $Cx43^{+/+}$ mice in N and CH conditions (white and black columns respectively). Pulmonary artery acceleration time (PAAT) and velocity time integral (VTI) is indicated on each picture. Quantification of PAAT is shown in b) and quantification of the heart rate is shown in c). n is the number of mice. Data represent means ± S.E.M. * $P<0.05$.

Figure S8. Capillary density and apoptosis in right ventricles from $Cx43^{+/-}$ mice compared with $Cx43^{+/+}$ mice in N and CH conditions. a) Capillaries are visualized by CD31 staining in red in right ventricles from $Cx43^{+/-}$ mice compared with $Cx43^{+/+}$ mice in N and CH conditions. Nuclei of cardiomyocytes are labelled in blue with DAPI. b) is the quantification of the capillary density from the right ventricles of $Cx43^{+/+}$ and $Cx43^{+/-}$ mice in N and CH conditions (white and black columns respectively). n is the number of areas analyzed from 4 to 5 mice from each group. c) TUNEL methodology was used to detect apoptotic cells (in red) in right ventricles sections from heart of $Cx43^{+/+}$ and $Cx43^{+/-}$ mice in N and CH conditions. Mouse colon was used as a positive control (right picture in c). Nuclei of all cells are labelled with DAPI in blue.

Figure S9. Lung inflammation in intrapulmonary arteries from $Cx43^{+/-}$ mice compared with $Cx43^{+/+}$ mice in N and CH conditions. CD45 (a leukocyte marker) expression was assessed by immunofluorescent labelling in lung sections (red labelling) from $Cx43^{+/-}$ mice compared with $Cx43^{+/+}$ mice in N and CH conditions. White arrow heads highlight the red CD45 labelling. PA media is labelled with an antibody against α-smooth muscle actin (α-SMA) in green and nuclei are labelled with DAPI in blue. Top pictures are brightfield images of the bottom pictures. Scale bars are 50 µm.

Figure S10. Right ventricular systolic pressure following administration of bosentan alone or in the presence of carbachol in $Cx43^{+/-}$ mice compared with $Cx43^{+/+}$ mice in N and CH conditions. (a) shows quantification of the right ventricular systolic pressure in $Cx43^{+/+}$ mice in N and CH conditions (white and black columns respectively) after bosentan treatment (left

columns) and when carbachol (carb) was added (right columns, Bosentan + carb). (b) shows quantification of the right ventricular systolic pressure in $Cx43^{+/-}$ mice in N and CH conditions (white and black columns respectively) after bosentan treatment (left columns) and when carbachol (carb) was added (right columns, Bosentan + carb). n is the number of mice. * $P < 0.05$.

Figure S11. Expression of Cx37 and 40 mRNA in right and left heart ventricles from $Cx43^{+/-}$ mice compared with $Cx43^{+/+}$ mice in N and CH. mRNAs were assessed by quantitative PCR for Cx37 in a and Cx40 in b. Data represent means ± SEM. n is the number of mice.

References

1. Freund-Michel V, Cardoso Dos Santos M, Guignabert C, Montani D, Phan C, Coste F, Tu L, Dubois M, Girerd B, Courtois A, Humbert M, Savineau JP, Marthan R, Muller B. Role of Nerve Growth Factor in Development and Persistence of Experimental Pulmonary Hypertension. *Am J Respir Crit Care Med* 2015; 192: 342-355.
2. Rodat-Despoix L, Aires V, Ducret T, Marthan R, Savineau JP, Rousseau E, Guibert C. Signalling pathways involved in the contractile response to 5-HT in the human pulmonary artery. *Eur Respir J* 2009; 34: 1338-1347.
3. Parpaite T, Cardouat G, Mauroux M, Gillibert-Duplantier J, Robillard P, Quignard JF, Marthan R, Savineau JP, Ducret T. Effect of hypoxia on TRPV1 and TRPV4 channels in rat pulmonary arterial smooth muscle cells. *Pflugers Arch* 2016; 468: 111-130.
4. Reaume AG, de Sousa PA, Kulkarni S, Langille BL, Zhu D, Davies TC, Juneja SC, Kidder GM, Rossant J. Cardiac malformation in neonatal mice lacking connexin43. *Science* 1995; 267: 1831-1834.

5. Geneau G, Defamie N, Mesnil M, Cronier L. Endothelin1-induced Ca(2+) mobilization is altered in calvarial osteoblastic cells of Cx43(+/-) mice. *J Membr Biol* 2007; 217: 71-81.
6. Dubois M, Delannoy E, Duluc L, Closs E, Li H, Toussaint C, Gadeau AP, Godecke A, Freund-Michel V, Courtois A, Marthan R, Savineau JP, Muller B. Biopterin metabolism and eNOS expression during hypoxic pulmonary hypertension in mice. *PLoS One* 2013; 8: e82594.
7. Fresquet F, Pourageaud F, Leblais V, Brandes RP, Savineau JP, Marthan R, Muller B. Role of reactive oxygen species and gp91phox in endothelial dysfunction of pulmonary arteries induced by chronic hypoxia. *Br J Pharmacol* 2006; 148: 714-723.
8. Xie F, Xiao P, Chen D, Xu L, Zhang B. miRDeepFinder: a miRNA analysis tool for deep sequencing of plant small RNAs. *Plant Mol Biol* 2012.

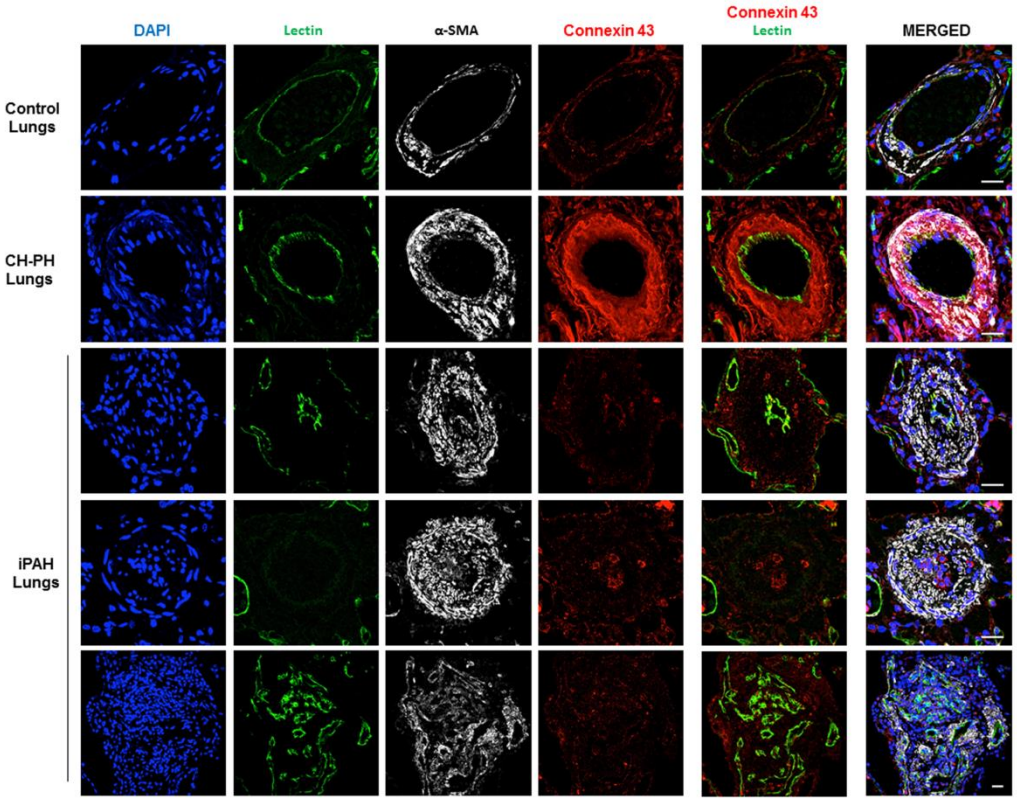
DAPI
Lectin
α-SMA
Connexin 43
Connexin 43
Lectin
MERGED
Control Lungs
CH-PH Lungs
iPAH Lungs

FIGURE S1

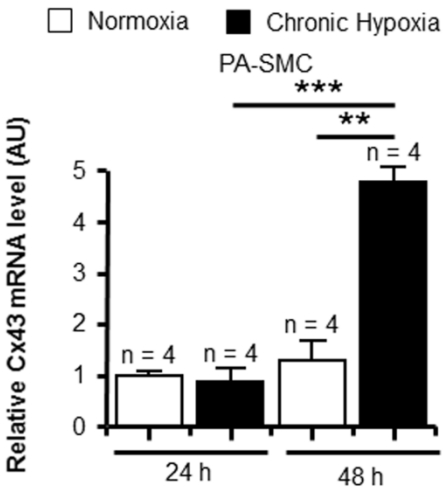
Normoxia
Chronic Hypoxia
PA-SMC
***
**
n = 4
n = 4
n = 4
n = 4
Relative Cx43 mRNA level (AU)
0
1
2
3
4
5
24 h
48 h

FIGURE S2

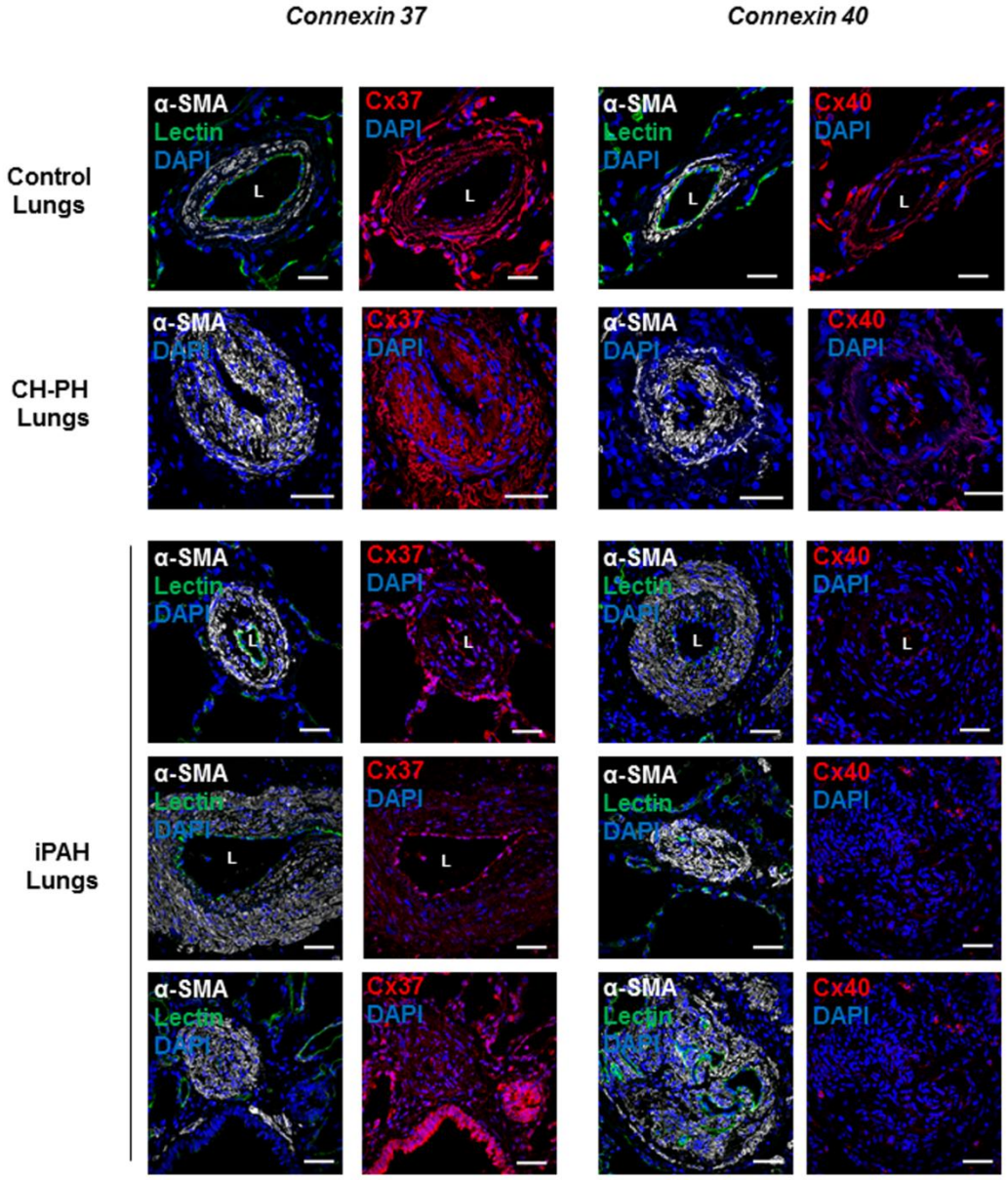
Connexin 37
Connexin 40
Control Lungs
CH-PH Lungs
iPAH Lungs
α-SMA
Lectin
DAPI
Cx37
Cx40
L

FIGURE S3

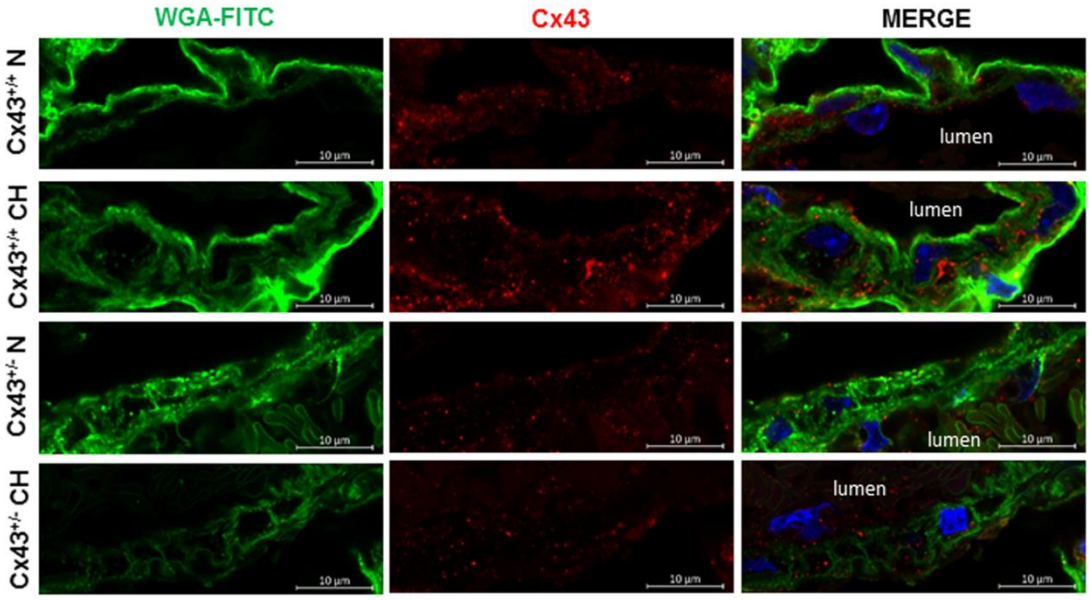
WGA-FITC
Cx43
MERGE
Cx43+/+ N
Cx43+/+ CH
Cx43+/- N
Cx43+/- CH
lumen
lumen
lumen
lumen
10 µm

FIGURE S4

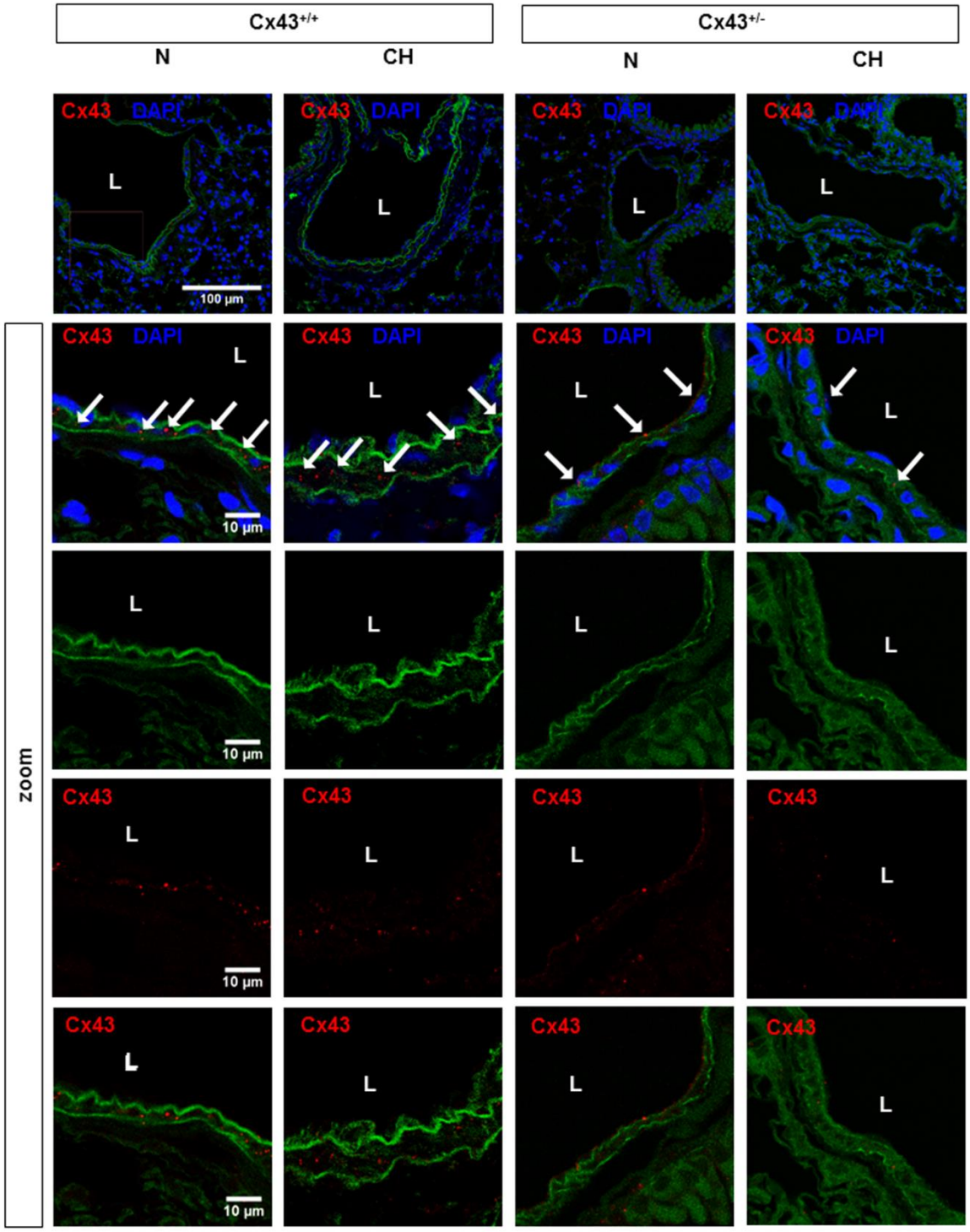

FIGURE S45

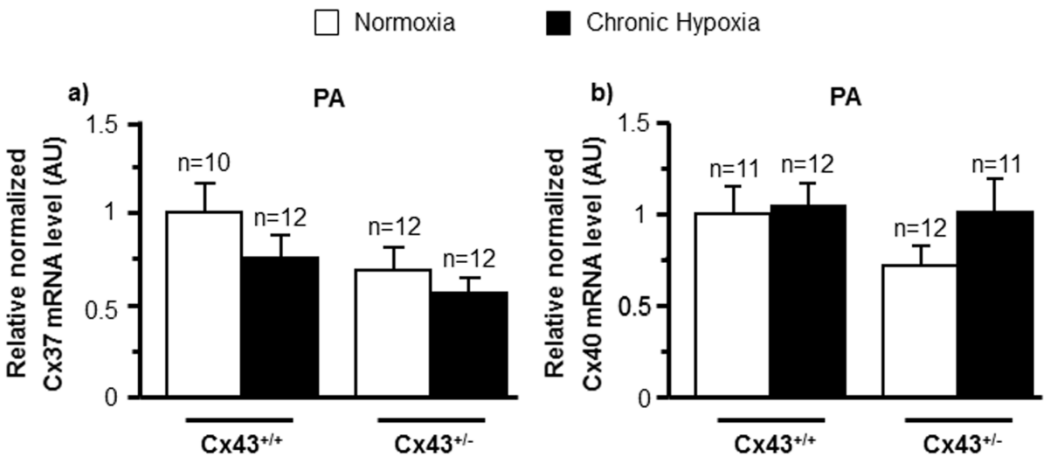
Normoxia
Chronic Hypoxia
a)
PA
Relative normalized Cx37 mRNA level (AU)
1.5
1
0.5
0
n=10
n=12
n=12
n=12
Cx43+/+
Cx43+/-
b)
PA
Relative normalized Cx40 mRNA level (AU)
1.5
1
0.5
0
n=11
n=12
n=12
n=11
Cx43+/+
Cx43+/-

FIGURE S6

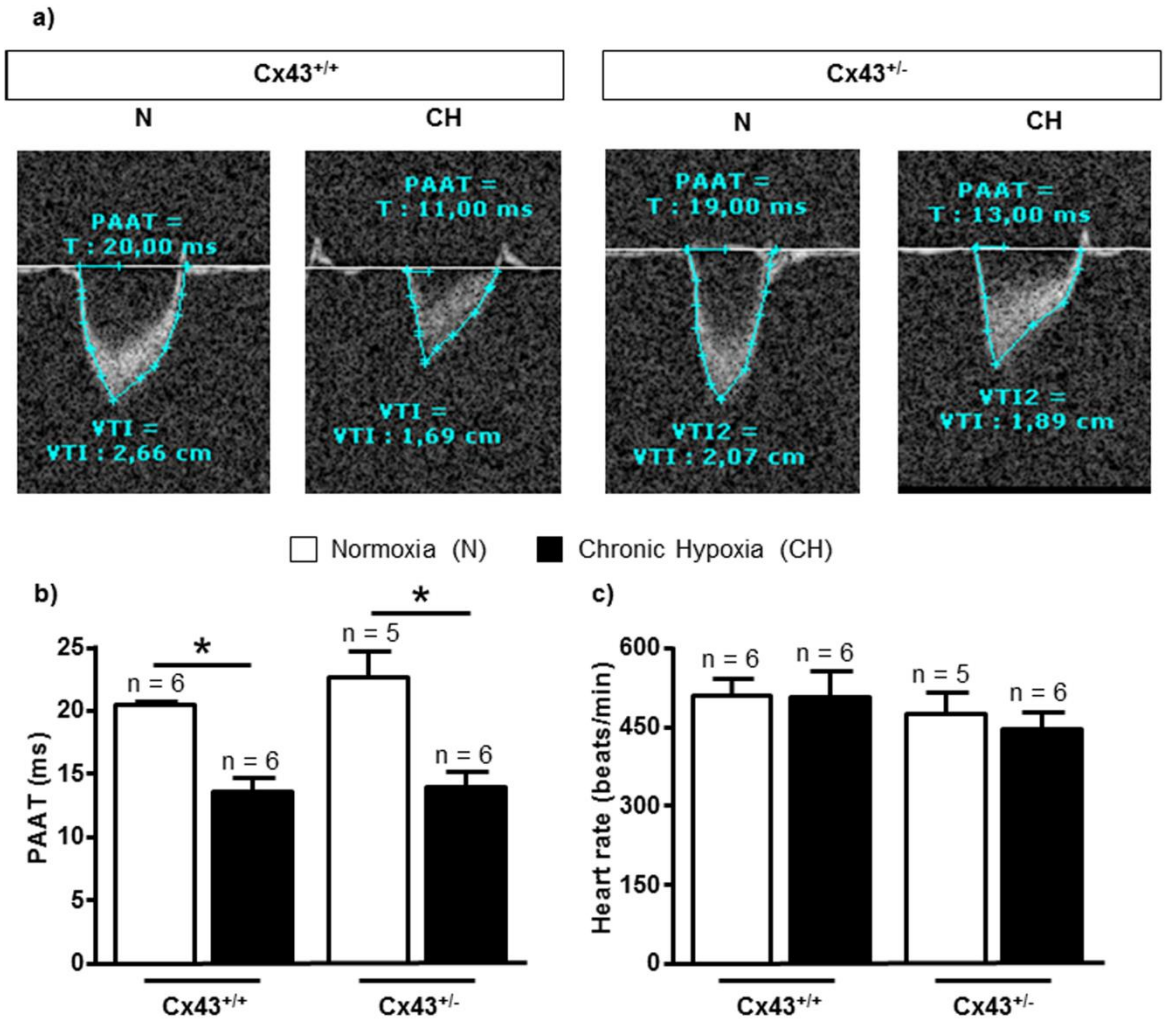
a)
Cx43+/+
Cx43+/-
N
CH
N
CH
PAAT =
T : 20,00 ms
VTI =
VTI : 2,66 cm
PAAT =
T : 11,00 ms
VTI =
VTI : 1,69 cm
PAAT =
T : 19,00 ms
VTI2 =
VTI : 2,07 cm
PAAT =
T : 13,00 ms
VTI2 =
VTI : 1,89 cm
Normoxia (N)
Chronic Hypoxia (CH)
b)
PAAT (ms)
25
20
15
10
5
0
n = 6
n = 6
n = 5
n = 6
*
*
Cx43+/+
Cx43+/-
c)
Heart rate (beats/min)
600
450
300
150
0
n = 6
n = 6
n = 5
n = 6
Cx43+/+
Cx43+/-

FIGURE S7

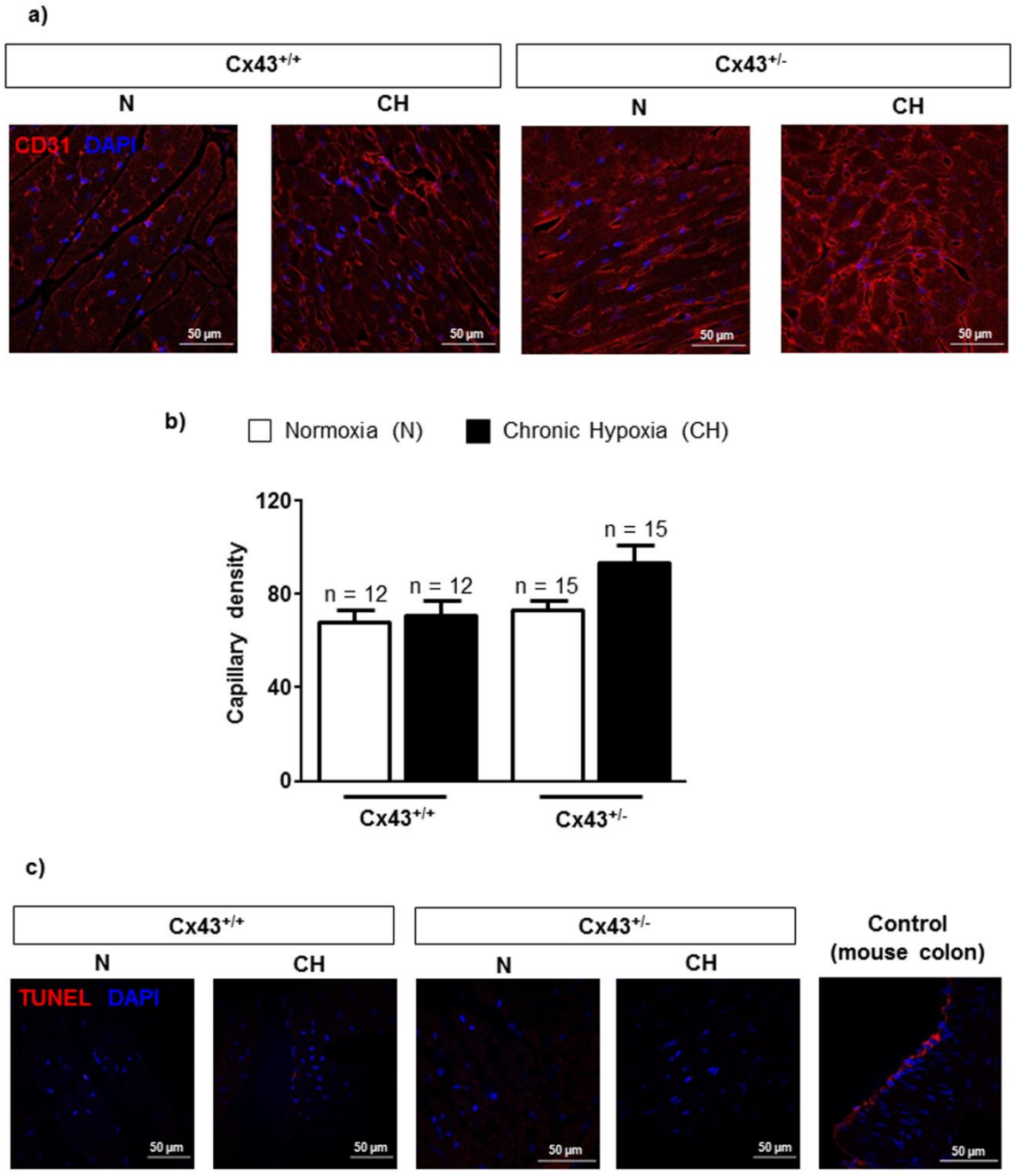
a)
Cx43+/+
Cx43+/-
N
CH
N
CH
CD31 DAPI
50 µm
50 µm
50 µm
50 µm
b)
Normoxia (N)
Chronic Hypoxia (CH)
Capillary density
120
80
40
0
n = 12
n = 12
n = 15
n = 15
Cx43+/+
Cx43+/-
c)
Cx43+/+
Cx43+/-
Control
(mouse colon)
N
CH
N
CH
TUNEL DAPI
50 µm
50 µm
50 µm
50 µm
50 µm

FIGURE S8

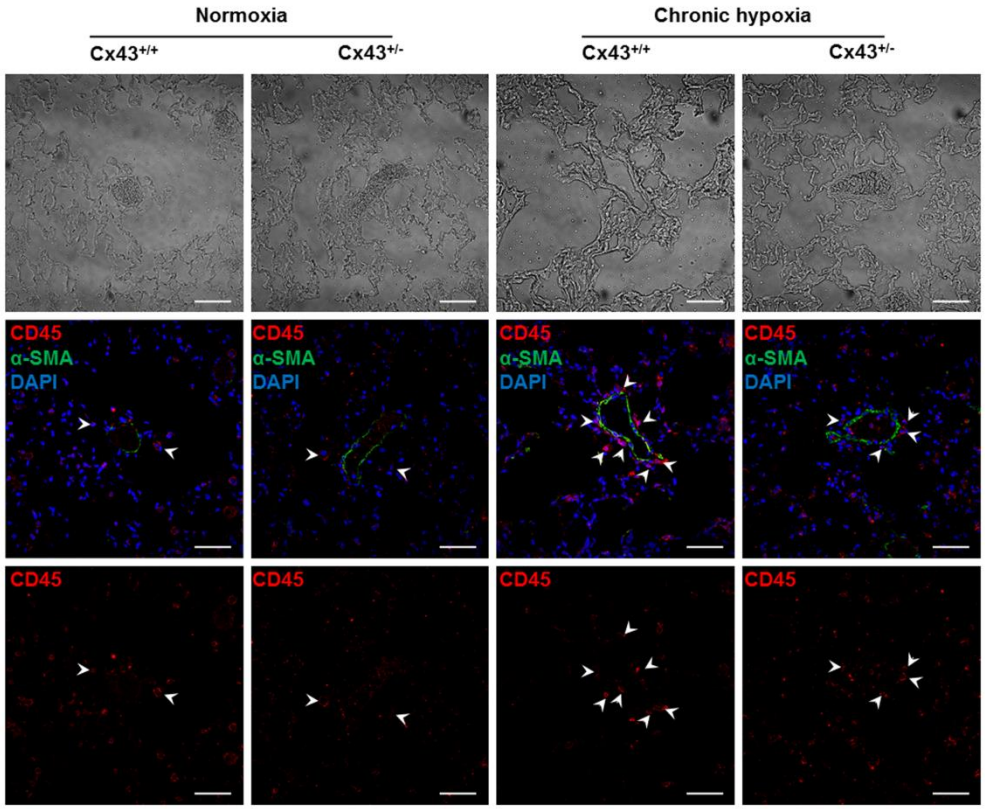

FIGURE S9

Scale bar 50 μm

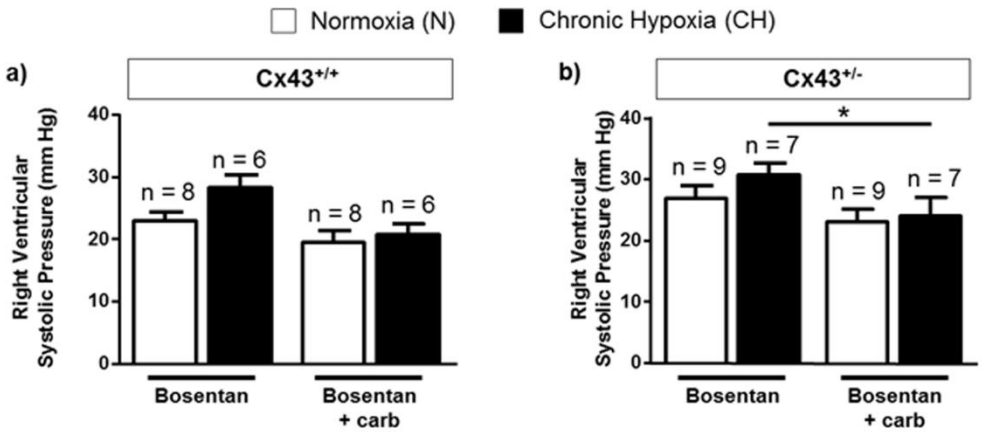
Normoxia (N)
Chronic Hypoxia (CH)
a)
Cx43+/+
Right Ventricular Systolic Pressure (mm Hg)
40
30
20
10
0
n = 8
n = 6
n = 8
n = 6
Bosentan
Bosentan + carb
b)
Cx43+/-
*
n = 9
n = 7
n = 9
n = 7
Bosentan
Bosentan + carb

FIGURE S10

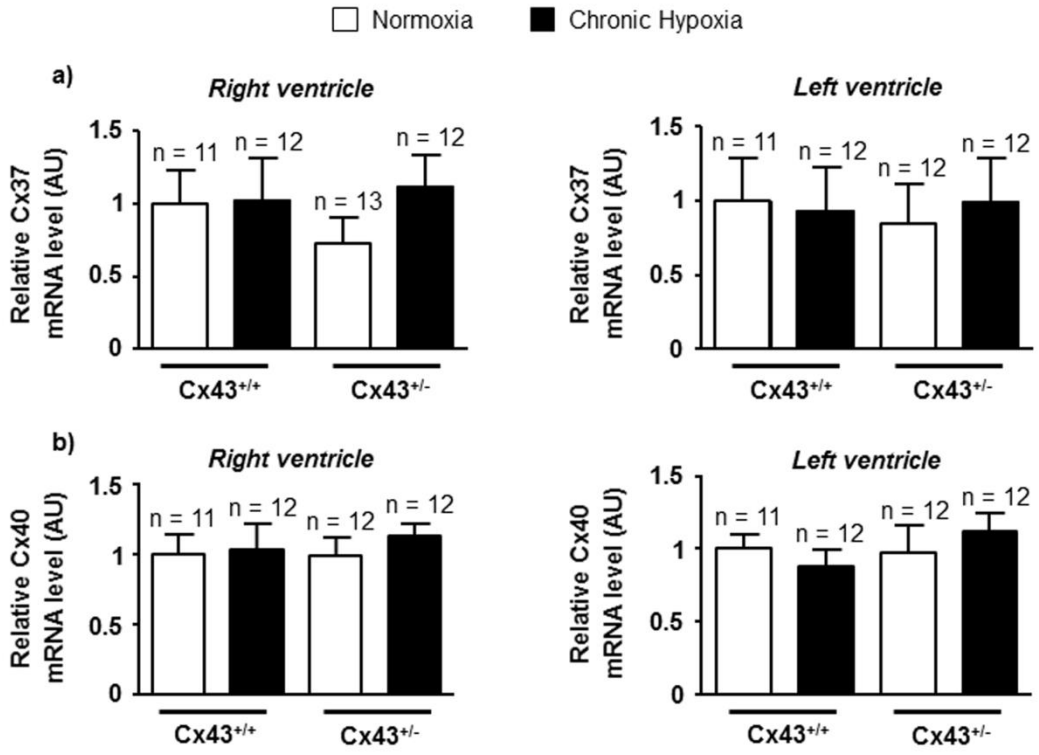
Normoxia
Chronic Hypoxia
a)
Right ventricle
Left ventricle
Relative Cx37 mRNA level (AU)
1.5
1
0.5
0
n = 11
n = 12
n = 13
n = 12
Cx43+/+
Cx43+/-
b)
Right ventricle
Left ventricle
Relative Cx40 mRNA level (AU)
n = 11
n = 12
n = 12
n = 12

FIGURE S911